

# Recent Advances in Hydrotreating of Pyrolysis Bio-Oil and Its Oxygen-Containing Model Compounds

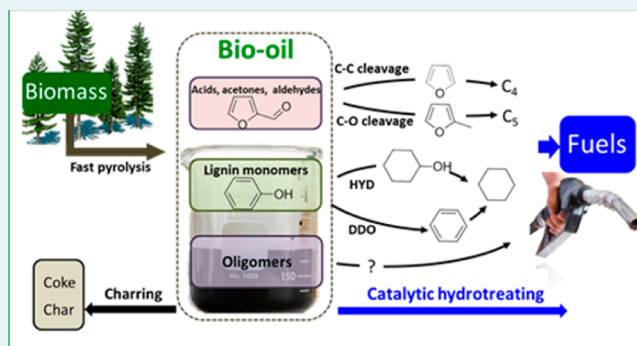
Huamin Wang,<sup>†</sup> Jonathan Male,<sup>†</sup> and Yong Wang<sup>\*,†,‡</sup>

<sup>†</sup>Pacific Northwest National Laboratory, P.O. Box 999, 902 Battelle Boulevard, Richland, Washington 99352, United States

<sup>‡</sup>Voiland School of Chemical Engineering and Bioengineering, Washington State University, Pullman, Washington 99163, United States

**ABSTRACT:** Considerable worldwide interest exists in discovering renewable energy sources that can substitute for fossil fuels. Lignocellulosic biomass, the most abundant and inexpensive renewable feedstock on the planet, has a great potential for sustainable production of fuels, chemicals, and carbon-based materials. Fast pyrolysis integrated with hydrotreating, one of the simplest, most cost-effective, and most efficient processes to convert lignocellulosic biomass to liquid hydrocarbon fuels for transportation, has attracted significant attention in recent decades. However, effective hydrotreating of pyrolysis bio-oil presents a daunting challenge to the commercialization of biomass conversion via pyrolysis-hydrotreating. Specifically, the development of active, selective, and stable hydrotreating catalysts is problematic due to the poor quality of current pyrolysis bio-oil feedstock (i.e., high oxygen content, molecular complexity, coking propensity, and corrosiveness). Significant research has been conducted to address the practical issues and provide fundamental understanding of hydrotreating and hydrodeoxygenation (HDO) of bio-oils and their oxygen-containing model compounds, including phenolics, furans, and carboxylic acids. A wide range of catalysts have been studied, including conventional Mo-based sulfide catalysts and noble metal catalysts. Noble metal catalysts have been the primary focus of recent research because of their excellent catalytic performances and because they do not require the use of environmentally unfriendly sulfur. Recently, the reaction mechanisms of the HDO of model compounds on noble metal catalysts and their efficacy for hydrotreating or stabilization of bio-oil have been reported. This review provides a survey of relevant literature, published over the past decade, reporting advances in the understanding of the HDO chemistry of bio-oils and their model compounds, mainly on noble metal catalysts.

**KEYWORDS:** biomass, lignocellulose, pyrolysis bio-oil, hydrodeoxygenation, catalysts, noble metal catalysts, model compounds



## 1. INTRODUCTION

Most activities in modern society depend heavily on fossil resources (e.g., oil, natural gas, and coal). In 2010, fossil fuels accounted for 87% of energy consumed worldwide and 87 and 92% of energy consumed in the United States and China, respectively.<sup>1</sup> Increased utilization of fossil fuels is an international concern due to dwindling fossil-fuel resources,<sup>2–4</sup> environmental consequences of CO<sub>2</sub> emission from fossil fuels,<sup>5</sup> and economic and political problems resulting from uneven distribution of fossil-fuel resources. Significant research has been conducted worldwide to discover alternative energy sources, which should be renewable and carbon-neutral and have the potential to replace fossil fuels in the current energy production and conversion system.<sup>6</sup> Attractive resources include solar, wind, hydroelectric, geothermal, and biomass. Of these, biomass is the only sustainable resource for the production of fuels, chemicals, and carbon-based materials, especially for liquid hydrocarbon fuels for transportation.<sup>6,7</sup> Currently, oil is the major resource (94%) used in the transportation energy sector; in 2009, it accounted

for 69% of oil consumption and 29% of total energy consumption in the United States.<sup>8</sup> New strategies must be developed for the efficient and large-scale production of fuels from biomass sources that can be used in current energy system.

Lignocellulosic biomass (e.g., woods, grass, energy crop, and agricultural waste) is currently the most inexpensive and abundant source of plant biomass.<sup>6,9</sup> It is desirable to convert the whole energy in the lignocellulosic biomass to transportation fuels using existing infrastructure.<sup>10</sup> Three primary routes have attracted the most attention:<sup>6,7,11–13</sup> gasification to synthesis gas (CO and H<sub>2</sub>) followed by Fischer–Tropsch synthesis to liquid hydrocarbons (biomass to liquids, BTL);<sup>6,7,14,15</sup> pyrolysis or liquefaction to bio-oils followed by catalytic upgrading to hydrocarbon fuels;<sup>6,7,16–21</sup> and pretreatment-hydrolysis to aqueous sugars followed by aqueous-phase

Received: January 29, 2013

Revised: April 5, 2013

Published: April 9, 2013

catalytic processing or fermentation to hydrocarbon fuels.<sup>6,7,22,23</sup> The first two routes can utilize whole lignocellulosic biomass, but the third route can only utilize the cellulose and hemicellulose portion of lignocellulosic biomass. Among these routes, pyrolysis integrated with upgrading is the simplest and most cost-effective,<sup>24</sup> and, thus, the resulting bio-oils (pyrolysis oils) have been identified as the cheapest renewable liquid fuels.<sup>18</sup> Pyrolysis is the thermal decomposition of lignocellulose in the absence of oxygen at temperatures between 648 and 800 K. During pyrolysis, a number of reactions occur (e.g., depolymerization, dehydration, and C–C bond cleavage), leading to the formation of a complex mixture of >200 oxygenated compounds.<sup>18,19,21,25</sup> Advanced fast pyrolysis can produce bio-oils in high yields (up to 80 wt % of dry feed) with up to 70% of the energy stored in the biomass feedstocks retained in the final bio-oils.<sup>6,7</sup> Catalytic fast pyrolysis, wherein fast pyrolysis is integrated with a catalysis process to upgrade the pyrolysis vapor with similar operation conditions, can lead to a higher quality bio-oil—but at the expense of product yield.<sup>26–36</sup> Another variation, hydro-pyrolysis, is fast pyrolysis conducted in the presence of reactive gases such as H<sub>2</sub>.<sup>37,38</sup> Both catalytic fast pyrolysis and hydro-pyrolysis suffer higher operational complexity; however, both have the potential to produce hydrocarbons directly from biomass or produce higher quality bio-oils more amenable for the subsequent upgrading process. Recently, several excellent reviews on pyrolysis have been published.<sup>18,19,21,39</sup> In addition, a number of fast pyrolysis technologies have been commercialized,<sup>21,39</sup> including a small portable pyrolysis reactor being commercially developed for the densification of biomass close to its location.<sup>13,18</sup>

Although bio-oil can be produced in a simple and efficient way, its properties result in multiple significant problems during its utilization as transportation fuels in standard equipment such as combustion boilers, engines, and turbines constructed for use of oil-derived fuels.<sup>18</sup> Primarily, the high oxygen content of bio-oils, usually 20 to 50 wt %, leads to different physical and chemical properties and combustion behaviors between bio-oils and petroleum fuels.<sup>40,41</sup> Specifically, the low heating value, poor stability, poor volatility, high viscosity, and corrosiveness of bio-oils limit their utilization as transportation fuels.<sup>18,40</sup> Catalytic fast pyrolysis and hydro-pyrolysis can produce bio-oil with improved quality; however, similar issues still exist, although to a lesser extent. Therefore, extensive oxygen removal is required for upgrading bio-oils to liquid transportation fuels with similar properties to petroleum fuels (e.g., high energy density, high stability, and high volatility).

Several approaches have been studied to upgrade bio-oils (see Figure 1) including hydrotreating,<sup>7,17,20,42</sup> zeolite upgrading,<sup>7,43–48</sup> and aqueous-phase processing.<sup>49</sup> Further, additional technologies (e.g., condensation and fractionation) have been

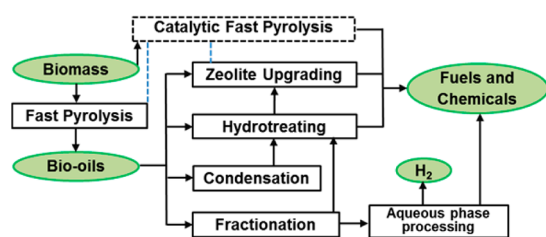


**Figure 1.** Pyrolysis-upgrading routes for the conversion of biomass into liquid fuels and chemicals.

used to make bio-oil feedstock more amenable to these upgrading processes. These processes have also been combined to achieve better hydrocarbon yields and deeper oxygen removal.<sup>50</sup> Hydrotreating is the most common route to upgrading bio-oil, involving oxygen removal through hydrodeoxygenation (HDO) to form hydrocarbons and H<sub>2</sub>O with saturation of double bonds or aromatic rings by hydrogenation.<sup>16,41</sup> Hydrotreating takes place between 400 and 773 K under high-pressure hydrogen in the presence of supported transition metal or their sulfide catalysts.<sup>17,42</sup> Zeolite upgrading, a route similar to the catalytic cracking in petroleum refining, treats bio-oils using cracking catalysts (normally acidic zeolites) at atmospheric pressure without the requirement of hydrogen at between 623 and 773 K.<sup>7,43–48</sup> In zeolite upgrading, oxygen in the oxygenated compounds of bio-oils is mainly removed as CO, CO<sub>2</sub>, and H<sub>2</sub>O and the products obtained are mostly aromatic and aliphatic hydrocarbons via a number of reactions (e.g., dehydration, cracking, and aromatization).<sup>7,45</sup> However, this method suffers from low hydrocarbon yield because of the high yield to coke and dealumination of zeolite due to the water in bio-oils, which consequently deactivates the catalyst. Another approach, aqueous-phase processing, can treat some fraction of bio-oil to form hydrocarbons and hydrogen. Specifically, bio-oils are first separated by the addition of water and then the aqueous fraction is treated in an aqueous-phase reforming process to produce hydrogen<sup>49</sup> or in an aqueous-phase dehydration/hydrogenation process to produce alkanes.<sup>49,50</sup>

As noted previously, in recent decades bio-oil hydrotreating has attracted the most attention and is the most common method to remove oxygen from bio-oils. Hydrotreating is one of the key processes in modern oil refining; it involves hydrodesulfurization (HDS), hydrodenitrogenation (HDN), and HDO to remove the sulfur, nitrogen, and oxygen heteroatoms, respectively, often accompanying hydrogenation (saturation) of olefins and aromatics in petroleum feedstocks.<sup>51,42</sup> Less attention has been paid to HDO as compared to HDS during petroleum upgrading research because the low oxygen content in oils (<0.3 wt %) causes much less environmental concern.<sup>42</sup> However, the high oxygen content in bio-oils (20 to 50 wt %) makes HDO a critical research topic in bio-oil upgrading. During HDO, the O content in bio-oils is reduced by saturating C=O bond, cleaving C–O bond, and forming C–H bond (deoxygenation); therefore, to reduce the O content in bio-oils, C=O bonds and aromatic rings are saturated by hydrogenation and other reactions occur (e.g., C–C bond hydrogenolysis or cracking, isomerization, and hydration). Deoxygenation is preferable to hydrogenation to minimize H<sub>2</sub> consumption and maintain a high aromatic content (and therefore octane number). HDO increases the energy density and stability but reduces the viscosity of fuels.<sup>7</sup> The highly reactive nature of the bio-oil has high propensity for coke formation during hydrotreating, resulting in severe reactor plugging and catalyst deactivation. Therefore, an additional hydrotreating stage at a lower temperature is recommended to stabilize bio-oil.<sup>17,52</sup>

Supported CoMo- and NiMo-based sulfide catalysts, which have served as industrial hydrotreating catalysts in refining for decades, have also been used in HDO of bio-oil with a drawback of adding environmentally unfriendly sulfur to the feed to keep catalyst from deactivating. In addition, noble metals (e.g., Ru, Pd, Pt, Re, and Rh), base metals (e.g., Ni and Cu), and metal phosphides and carbides have been used recently in HDO, however, mostly for HDO of model

compounds of bio-oils. Acids, in either aqueous form or solid form, have been combined with metals to achieve faster HDO by bifunctional catalysis. Significant challenges still exist in the rational design of more effective HDO catalysts and processes for upgrading bio-oil in a simpler process with higher reaction rates, lower H<sub>2</sub> requirement, higher carbon yield, and improved catalyst life.

Over the past 30 years, a wider range of studies have been reported in the literature regarding fundamental and practical assessments of hydrotreating bio-oils and their oxygen-containing model compounds over a variety of catalysts. A review by Furimsky focused on the chemistry (mechanisms and kinetics) of the HDO of representative compounds (mainly furans and phenols) on Mo-based sulfide catalysts and the role of HDO in hydrotreating of traditional oils.<sup>42</sup> A review by Elliott in 2007 provided a very detailed summary of research efforts on processing actual bio-oil products.<sup>17</sup> Other recent reviews also discussed hydroprocessing of actual bio-oils,<sup>20,41</sup> and more general reviews have highlighted the importance of the HDO of bio-oils.<sup>6,7</sup>

This review focuses on literature from the past decade relevant to furthering the understanding of HDO chemistry of bio-oils and their model compounds on mainly non-sulfide metal catalysts. HDO on sulfide catalyst will be disseminated for the purpose of comparison, and the most recent advances in HDO of actual bio-oil will be summarized.

## 2. BIO-OIL AND ITS MAJOR OXYGEN-CONTAINING COMPONENTS

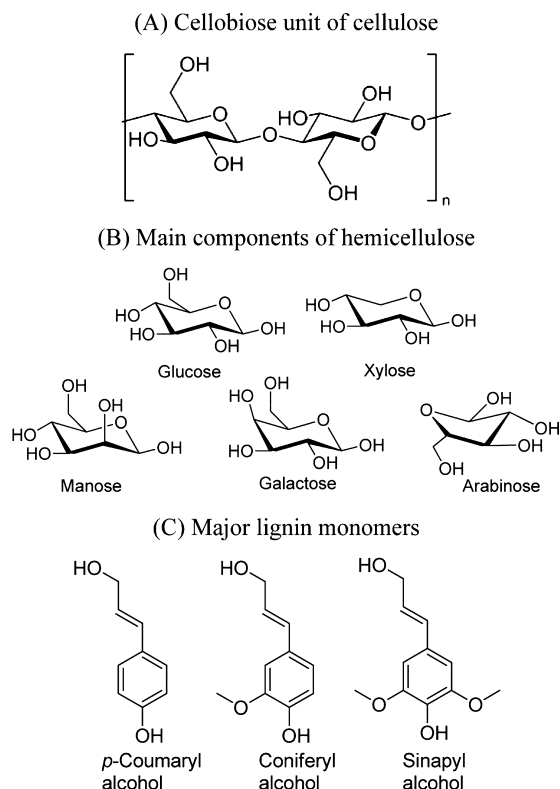
Bio-oils from fast pyrolysis of biomass are multicomponent mixtures of a large number of oxygenated compounds derived from lignocellulosic biomass feedstocks (e.g., woods, grasses, energy crops, agricultural wastes, and forest wastes). The structured portion of lignocellulosic biomass is composed of cellulose (28 to 55%), hemicellulose (17 to 35%), and lignin (17 to 35%), which are oxygen-containing organic polymers. The weight percentage of these three major components varies in different biomass species, as shown in Table 1 for pinewood, poplarwood, and switchgrass.<sup>7,53</sup> Other minor biomass components include organic extractives and inorganic minerals.

**Table 1. Typical Lignocellulose Content of Some Biomass Species**

biomass species	lignocellulose content (wt %)		
	cellulose	hemicellulose	lignin
pinewood <sup>a</sup>	46–50	19–22	21–29
poplarwood <sup>b</sup>	40–46	17–23	21–28
switchgrass <sup>b</sup>	28–37	23–29	17–20

<sup>a</sup>Based on data reported in ref 7. <sup>b</sup>Based on the data reported in ref 53.

The structure of cellulose, hemicellulose, and lignin are shown in Figure 2. Cellulose is a high-molecular-weight linear polymer of  $\beta$ -D-anhydroglucopyranose units (AGUs,  $\sim$ 10,000 AGUs for cellulose chain in wood), and its basic repeat unit consists of two AGUs, called a cellobiose unit, as shown in Figure 2A.<sup>54</sup> Cellulose degrades at  $\sim$ 573 K to produce levoglucosan and other anhydrocellulose.<sup>55</sup> Hemicellulose is derived from several sugars in addition to glucose, especially xylose but also mannose, galactose, and arabinose (Figure 2B), all of which are highly substituted with acetic acid. Hemicellulose consists of shorter and branched chains ( $\sim$ 200 sugar

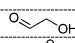
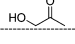
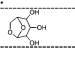
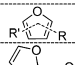
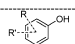
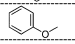
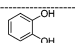


**Figure 2.** Structure of different lignocellulosic biomass fractions: (A) cellulose, (B) hemicellulose, (C) lignin.

units). Decomposition of hemicellulose at between 473 and 533 K leads to acetic acid and anhydrocellulose.<sup>19</sup> Lignin, an amorphous, highly branched, and substituted polymer, consists of an irregular array of variously “hydroxyl”- and “methoxyl”-substituted phenylpropane units with relatively hydrophobic and aromatic nature. Three representative units, *p*-coumaryl, coniferyl, and sinapyl, are shown in Figure 2C. Lignin structure and properties are different for different feedstocks. Lignin decomposes at between 553 and 773 K to form oligomers and monomers of polysubstituted phenols via the cleavage of ether and C–C linkages.<sup>19,56</sup>

Lignocellulosic biomass decomposes during fast pyrolysis to produce a wide range of products including vapors, aerosols, and charcoal-like char. Cooling and condensation of the vapors and aerosols results in the formation of a dark brown liquid referred to as bio-oil. The bio-oil yields from wood are in the range of 72 to 80 wt %, depending on the feedstock and process used.<sup>19,21</sup> Other products include noncondensable gases (10 to 20 wt %) and solid char (15 to 25 wt %).<sup>19,21</sup> Advanced fast pyrolysis to achieve high liquid yield requires careful pretreatment of biomass (drying and milling), high heating rates, high heat transfer rate, well-controlled temperature (698 to 773 K), short residence time (0.5 to 5 s), and rapid cooling and quenching of pyrolysis vapor.<sup>19,21,57</sup> The reaction during fast pyrolysis involves rapid depolymerization and fragmentation of the cellulose, hemicellulose, and lignin to their primary decomposed molecules, as mentioned above, and some volatiles. Subsequent reactions including isomerization, dehydration, repolymerization/condensation, decomposition, and C–C bond cleavage occur during pyrolysis and rapid quenching, leading to a very complicated mixture of >200 organic compounds. This product is not thermodynamically

Table 2. Major Compounds in Typical Wood Pyrolysis Bio-Oils<sup>a</sup>

Catalog	Typical Compounds	Structure <sup>b</sup>	
Water	Water	H <sub>2</sub> O	
Simple oxygenates	Acids	acetic acid, formic acid, propanoic acid, methyl-propanoic acid, butanoic acid, methyl butanoic acid, pentanoic acid, glycolic acid, etc.	
	Esters	methyl acetate, methyl formate, methyl propionate, butyrolactone, dimethyl pentanedioate; etc.	
	Alcohols	butane-2,3-diol, methanol, ethanol, 2-propene-1-ol, isobutanol; ethylene glycol etc.	
	Ketones	acetone, 2-butanone, 2,3-butanedione; cyclopentanone; Methylcyclopentanone, 2-pentanone, cyclohexanone; 3-hexanone, methylcyclohexanone, cyclopentanedione; etc.	
Miscellaneous oxygenates	Aldehydes	2-butenal, glyoxal, formaldehyde; acetaldehyde; 2-propenal; 2-methyl-2-butenal, pentanal, benzaldehyde; etc.	
		glycolaldehyde	
		1-hydroxyl-2-propanone	
Sugars		methyl 2-oxopropanoate; 1-hydroxy-2-butanone; etc.	
		Levoglucofan	
Furans		glucose, fructose, D-xylose, D-arabinose, etc.	
		furan; methylfuran; dimethyl-furan;	
Hydro-carbons		furfural	
		2-furanone, 4-methyl-2-furanone, furfuryl alcohol, 2-acetyl furan; 5-methyl furfural; etc.	
	Alkene	hexane, methyl-propene, alkylated cyclohexene, etc.	
	Aromatics	toluene; xylene, ethylbenzene, naphthalene, etc.	
	Phenols	phenol, methylphenol, dimethylphenol	
	Anisoles	anisole	
		methyl-anisole, ethyl-anisole, etc.	
	Catechols	Catechol	
		methyl-catechol, ethyl-catechol, methoxycatechol, etc.	
	Phenolics	Guaiacols	guaiacol
	methyl-guaiacol, ethyl-guaiacol, eugenol, etc.		
	Syringols	syringol, methyl-syringol, ethyl-syringol, propyl-syringol, 4-propenylsyringol, etc.	
	Others	vanillin, vanillic acid, sinapaldehyde, syringaldehyde, acetosyringone, etc.	
High-molecular-weight species	Dimmer, trimmer, and oligomer of cellulose, hemicellulose, and lignin pyrolysis products.		

<sup>a</sup>Based on results in refs 58–62. <sup>b</sup>R, R' = H or CH<sub>3</sub>.

equilibrated, and therefore its chemical composition tends to change during storage.

Table 2 lists the major compounds in typical bio-oils from wood, based on the detailed analysis reported in various literatures.<sup>58–62</sup> Major groups of compounds include water, simple oxygenates (e.g., acids, esters, alcohols, ketones, aldehydes), miscellaneous oxygenates, sugars, furans (e.g., alkylated furan, furfural, hydroxymethyl furfural), phenolics (e.g., phenols, guaiacols, syringols), and high-molecular-weight compounds. Miscellaneous oxygenates, sugars, and furans are primarily derived from the cellulose and hemicellulose fractions of biomass, whereas phenolics are derived from the lignin component of biomass. Simple oxygenates (e.g., acids, esters, alcohols, ketones, and aldehydes) likely form from the decomposition of the miscellaneous oxygenates, sugars, and furans. High-molecular-weight compounds are primarily oligomers of phenolic compounds with molecular weights ranging from several hundred to as much as 5,000 or more.

The complicated components in bio-oils pose significant challenges for their further upgrading by hydrotreating. Traditional hydrotreating of petroleum-derived fuels (e.g., HDS to remove sulfur) is predominantly performed to remove sulfur from five-membered thiophenic heterocyclics (e.g., thiophene, benzothiophene, dibenzothiophene, and their alkylated compounds; including ~20 compounds with about ~1.0 to 1.8 wt % sulfur) in feedstocks.<sup>51</sup> Here, bio-oil has >20

oxygen-containing compounds, representing nearly all kinds of oxygenated organics and oxygen function groups, which can undergo intertwining interactions, making it extremely difficult to understand HDO catalysis reaction pathways, mechanisms, kinetics, and property–reactivity correlation of hydrotreating catalysts. In addition, extensive oxygen removal from bio-oil and some significant problems of bio-oil (e.g., high water content, acidity, and chemical instability) bring significant challenges for bio-oil hydrotreating catalysts and processes. Table 3 compares the typical compositions and physical properties of wood pyrolysis bio-oil and conventional fuel oil.<sup>18,40,42,61,62</sup> The presence of oxygen in almost every bio-oil component and, thus, the overall high oxygen content of bio-oil constitute the primary difference between bio-oil and petroleum-derived oils and are the cause of difficulties in bio-oil hydrotreating. Polymerization and condensation of bio-oils occur over time and can be accelerated by increasing temperature because of interactions of different components, especially highly reactive species (e.g., furfurals, guaiacols, and phenols),<sup>52,63</sup> leading to a high propensity of coke formation during hydrotreating and the consequent catalyst deactivation, and even plugging of catalyst bed.<sup>64</sup> Water, initially present in bio-oil with a high content (17–30 wt %) and also formed during hydrotreating, inhibits hydrotreating reactions by competitive adsorption on active sites and causes catalyst deactivation by modification of the catalyst structure.<sup>63,65</sup> Other

**Table 3. Typical Compositions and Physical Properties of Wood Pyrolysis Bio-Oil and Conventional Fuel Oil**

	wood pyrolysis bio-oil <sup>a</sup>	conventional fuel oil <sup>b</sup>
elementary analysis, wt %		
carbon	40–50	85
hydrogen	6.0–7.6	11–13
oxygen	36–52	0.1–1.0
sulfur	0.00–0.02	1.0–1.8
nitrogen	0.00–0.15	0.1
water, wt %	17–30	0.02–0.1
solid, wt %	0.03–0.7	1
pH	2.4–2.8	
viscosity (323 K), cP	13–30	180
HHV, MJ/kg	16–20	40
density, kg/m <sup>3</sup>	1.2–1.3	0.9–1.0

<sup>a</sup>Based on data reported in refs 40, 61, and 62. <sup>b</sup>Based on data reported in refs 18 and 42.

issues include deposition of inorganic species (e.g., alkali) on catalyst<sup>17</sup> and leaching of catalyst by bio-oil because of bio-oil acidity and corrosivity, which lead to the deactivation of hydrotreating catalysts. Catalytic fast pyrolysis and hydro-pyrolysis can produce bio-oil with improved quality (i.e., more favorable oxygen content, hydrocarbon content, acidity, and stability),<sup>33–39</sup> which is expected to alleviate challenges associated with downstream hydrotreating processes. However, even using catalytic fast pyrolysis and hydro-pyrolysis, a substantial amount of oxygen, reactive species, and water in the bio-oil leads to similar hydrotreating issues as described, although to a lesser extent. Rigorous data is lacking to demonstrate the advantages of hydrotreating bio-oil produced by catalytic fast pyrolysis or hydro-pyrolysis over bio-oil produced by conventional fast pyrolysis.

Improved hydrotreating processes and catalysts are required to efficiently upgrade bio-oils to transportation fuels. Extensive research has been conducted over the past decade, and significant advancement has been achieved in the fundamental understanding of the chemistry of reactions taking place during bio-oil hydrotreating and in the development of catalysts and processes to upgrade actual bio-oils and their model compounds.<sup>17,42</sup> Next, we will summarize the catalysts used in the HDO of bio-oil and provide a detailed review of the HDO chemistry of bio-oil model compounds.

### 3. HDO CATALYSTS

Various catalysts with different active phases, promoters, and supports have been studied in HDO of bio-oils and their oxygen-containing model compounds. Table 4 summarizes the catalysts in six groups: Mo-based sulfides, noble metals, base metals, metal phosphides, other metal catalysts, and bifunctional catalysts. Metals are present as zerovalent metal, sulfide, oxide, and others and in either mono- or bimetallic form. Supports include carbon, silica, alumina, zirconia, titania, amorphous silica–alumina, and various zeolites. Second function of bifunctional catalysts includes aqueous and solid acids.

Molybdenum sulfide, normally promoted by cobalt or nickel and supported on porous supports (e.g.,  $\gamma$ -Al<sub>2</sub>O<sub>3</sub>), has been widely used in modern hydrotreating processes. The reaction network, mechanism, and site requirement of HDS and HDN reactions on Mo-based sulfide catalysts have been studied extensively and are well-understood.<sup>51</sup> Mo-based sulfide

**Table 4. Catalysts for Bio-Oil Hydrotreating**

catalog	catalysts
Mo-based sulfides	bulk or supported MoS <sub>2</sub> , Ni–MoS <sub>2</sub> , and Co–MoS <sub>2</sub>
noble metals	supported Ru, Rh, Pd, Pt, Re, Pt–Rh, Pd–Rh, Pd–Cu, Pd–Fe, Pt–Re, and Ru–Mo; Ru, Pt, Rh nanoparticles
base metals	supported Cu, Ni, Ni–Cu, and Ni–Fe and Raney nickel
metal phosphides	supported Ni <sub>2</sub> P, MoP, NiMoP, CoMoP, Fe <sub>2</sub> P, WP, and RuP
other metal catalysts	bulk Ni–Mo–B; supported nitrides (Mo <sub>2</sub> N) and carbides (Mo <sub>2</sub> C); supported Mo-based oxide (MoO <sub>2</sub> , MoO <sub>3</sub> )
bifunctional catalysts	noble metal or base metal catalysts with aqueous acid including CH <sub>3</sub> COOH, H <sub>3</sub> PO <sub>4</sub> , and Nafion or solid acid including HZSM-5, H-Beta, H-Y, sulfated zirconia, and supported Nafion; metals including Pt, Pd, and Ni supported on acid solid including HZSM-5, H-Beta, HY, and bulk acidic salt

catalysts are also active for HDO and, therefore, are most commonly used for bio-oil hydrotreating.<sup>17</sup> Elliott et al.<sup>17,52</sup> reported that extensive oxygen removal from bio-oil (from ~45 to <1 wt %) was achieved to produce hydrocarbon with high yields by using a supported Mo-based sulfide catalyst in nonisothermal hydroprocessing. The HDO chemistry of Mo-based sulfide catalysts is also the most understood among the HDO catalysts; however, significant research on the reaction mechanism and nature of active site is still required.<sup>42</sup> To keep sulfide catalysts from deactivating, their sulfide form must be maintained during HDO by adding an appropriate source of sulfur (e.g., H<sub>2</sub>S) to the feed,<sup>65,66</sup> which deprives bio-oil of its advantage of low-sulfur content.

Recently, supported noble metals (e.g., Ru, Pd, Pt, and Rh), have attracted attention as effective non-sulfide-based hydrotreating catalysts. Studies of supported noble metals have focused primarily on the HDO of model compounds; however some studies have reported hydrotreating of actual bio-oil.<sup>52,67–70</sup> Compared to Mo-based sulfide catalysts, noble metals seem to show better performance regarding the hydrocarbon yield and deoxygenation level.<sup>67</sup> Of the supported noble metals, Ru catalyst is believed to be the most promising.<sup>67–69</sup> However, studies of HDO of model compounds indicated that HDO of phenols on noble metal catalyst (Rh, PtRh, and PdRh) favors a hydrogenation–deoxygenation path, whereas the reaction on Mo-based sulfide catalyst (CoMo and NiMo) favors a direct deoxygenation pathway under similar conditions,<sup>71</sup> leading to a concern of higher H<sub>2</sub> consumption by using noble metal catalysts than by using Mo-based sulfides. The reaction network of various bio-oil model compounds has been studied on noble metal catalysts. However, an intensive understanding is still lacking regarding the reaction mechanism, kinetics, and the nature of active site. Other metals (e.g., Ni, Cu, and their alloys) have also been tested in HDO of model compounds. Metal phosphides have been explored for HDO of phenolics (anisole and guaiacol).<sup>72,73</sup> A much higher guaiacol conversion on metal phosphide catalysts was seen than on commercial sulfide (CoMo) catalysts.<sup>73</sup> Ni<sub>2</sub>P was the most active catalyst for HDO among tested metal phosphides (i.e., Ni<sub>2</sub>P, Co<sub>2</sub>P, WP, MoP, and NiMoP).<sup>72,73</sup> Similar to sulfide catalysts, metal phosphide catalysts might be oxidized by water to form phosphate, which might cover the active sites and cause deactivation.<sup>72</sup> Recently, bifunctional catalysts, including a metal function and an acid function (either in aqueous phase such as H<sub>3</sub>PO<sub>4</sub>–H<sub>2</sub>O<sup>74</sup> or solid phase such as HZSM-5<sup>75</sup>), have shown a greatly improved HDO activity compared to metal catalyst alone.

Early studies have employed Mo-based sulfide with  $\text{Al}_2\text{O}_3$  as a support, which have shown appropriate pore structure and dispersion of active phase, and promotion effects for hydro-treating reactions. However,  $\text{Al}_2\text{O}_3$  is known to be responsible for coke formation due to its acidity and is unstable in the presence of large amounts of water.<sup>63,76</sup> To avoid these problems, neutral supports with better water tolerance (e.g., activated carbon) have been widely used in recent studies for hydrotreating of actual bio-oils<sup>52,67–69</sup> and model compounds.<sup>77</sup> In addition,  $\text{TiO}_2$  and  $\text{ZrO}_2$  have been used as supports with a better activity than  $\text{Al}_2\text{O}_3$ .<sup>78</sup> Further, mesoporous materials (e.g., MCM-41)<sup>79</sup> and zeolites (e.g., HBeta,<sup>80</sup> HY,<sup>81</sup> and HZSM-5<sup>82</sup>) have been utilized to prepare bifunctional catalysts or catalysts with enhanced diffusion properties. However, intensive investigation is still needed regarding the stability of  $\text{TiO}_2$ ,  $\text{ZrO}_2$ , and zeolite-supported catalysts during hydrotreating of actual bio-oil.

#### 4. HDO OF MODEL COMPOUNDS OF BIO-OIL: REACTION NETWORK, MECHANISM, AND KINETICS

The rational design of more effective HDO catalysts requires advancement in the fundamental understanding of the mechanism, kinetics, and site requirements for HDO reactions. Most studies for elucidation of HDO mechanism and kinetics have been conducted using model compounds including phenolics (phenols, anisole, and guaiacol), furans, and carboxylic acids, which are the major components in bio-oil. Reaction routes of HDO of model compounds have been investigated in recent studies, whereas kinetics and site requirements have received little attention. Both continuous-flow and batch reactor have been used for the HDO of model compounds. It is notable that the industrial process for bio-oil hydrotreating prefers continuous-flow reactor and that challenges exist in comparing data between continuous flow and batch reactors.

Cleavage of C–O bonds must occur for the removal of oxygen from oxygen-containing compounds. Some C–O bond strengths are listed in Table 5.<sup>42</sup> C–O bond strengths of the

**Table 5. Bond Dissociation Energies<sup>42</sup>**

bond	dissociation energy (kJ/mol)
R–OR	339
R–OH	385
Ar–OR	422
Ar–OH	468

OH group or RO group (aliphatic-oxygen) attached to an aromatic carbon (Ar–OH, phenols; or Ar–OR, aryl ethers) are about 83 kJ/mol greater than that attached to the aliphatic carbon (R–OH, alcohols; or R–OR, aliphatic ethers), respectively. This suggests that cleavage of C–O bonds attached to phenols and aryl ethers is more difficult than that of C–O bonds attached to alcohols and aliphatic ethers. Therefore, removal of oxygen from phenols or aryl ethers will be enhanced by first hydrogenation of the aromatic ring to the corresponding cycloalkane by converting of Ar–O bond to R–O bond. This also implies that a hydrogenation–deoxygenation route would be preferred in HDO of phenols or aryl ethers on catalysts with good hydrogenation activity (e.g., noble metal catalysts). Deoxygenation of alcohols (OH group attached to the aliphatic carbon) could occur by hydrogenolysis catalyzed by a metal catalyst or, alternately, by dehydration catalyzed by

an acid under milder conditions. Recent results showed that an acid function greatly promotes the deoxygenation activity of metal catalysts.

The sequence of C–O bond strength is also consistent with reported reactivity sequence of oxygenated groups on Mo-based sulfide catalysts under hydrotreating conditions. Grange et al.<sup>83</sup> compared the reactivity of oxygen-containing groups/compounds by showing the isoreactivity, which is the temperature at which the conversion rates reach a significant identical value on a sulfided CoMo/ $\text{Al}_2\text{O}_3$  catalyst (see Table 6). In addition, Grange et al. estimated that unsaturated double

**Table 6. Relative Reactivities of Oxygen-Containing Groups and Compounds<sup>83</sup>**

	activation energy (kJ/mol)	temp of isoreactivity (K)
ketone	50.2	476
carboxylic acid	108.9	556
methoxy phenol	113.0	574
4-methylphenol	140.7	613
2-ethylphenol	149.9	640

bonds (olefins), aliphatic alcohols, and ethers would react at even lower temperature than the ketonic group. Therefore, they suggested a low-temperature hydrotreatment would undergo hydrogenation of unsaturated double bonds (olefins, aldehydes, ketones) to stabilize the bio-oils, whereas deep HDO would require a higher temperature for the elimination of the phenolic and furanic oxygen-containing compounds. Similar reactivity ranking of oxygenated groups was also developed by Elliott<sup>17</sup> on the basis of the results from the literature. As shown in Figure 3, hydrogenation of olefins, aldehydes, and ketones

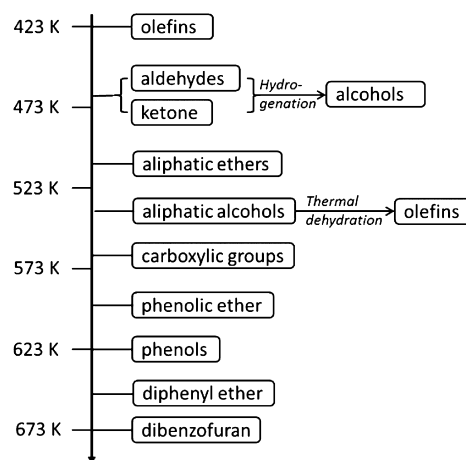


**Figure 3.** Reactivity scale of oxygenated groups under hydrotreatment conditions. Redrawn with permission from ref 17. Copyright 2007 American Chemical Society.

occurs at low temperatures. Alcohols are reacted from 423 to 473 K by catalytic hydrogenation but also by thermal dehydration to form olefins, while carboxylic acids, phenolic ethers, and phenols are reacted at from 573 to 623 K.

**4.1. HDO of Phenols.** Because functionalized phenols are the major components of bio-oils obtained from the lignin fraction of lignocellulosic biomass, compounds including phenol (and alkylated phenols) are the main model compounds in HDO studies. Studies on the HDO of phenol and cresol on sulfided CoMo catalyst established the basic reaction schemes

involving deoxygenation and hydrogenation reactions.<sup>42,84–88</sup> As shown in Figure 4, primary reactions of 4-methylphenol

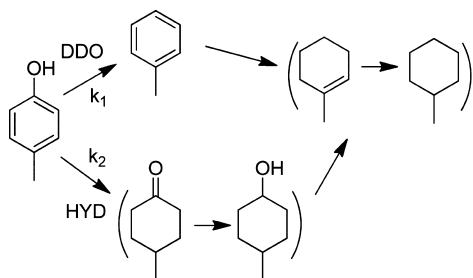


**Figure 4.** Reaction network of HDO of 4-methylphenol.

include two parallel routes: direct deoxygenation (C–O cleavage) to toluene (DDO route) and hydrogenation to 4-methyl-cyclohexanol (HYD route).<sup>84–88</sup> Subsequent hydrogenation of toluene or deoxygenation of 4-methylcyclohexanol occurs to produce the final product: methylcyclohexane. Kinetic studies showed a preference of the DDO route over the HYD route during the HDO of phenol and 3- or 4-methylphenol on CoMo sulfide catalysts.<sup>84,87</sup> Figure 5 summarizes the rate

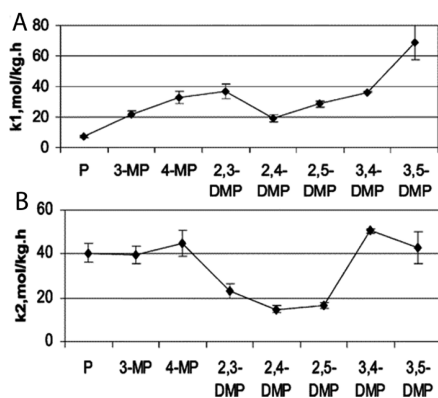


**Figure 5.** DDO rate constant ( $k_1$ , A) and HYD rate constant ( $k_2$ , B) of phenol (P), methylphenols (MP), and dimethylphenols (DMP) on sulfide CoMo catalyst. Reprinted with permission from ref 87. Copyright 2006 American Chemical Society.

constants of the two paths of the HDO of phenol and its methylated compounds measured in a continuous-flow reactor at 573 K and 2.85 MPa of hydrogen pressure over a sulfided CoMo/Al<sub>2</sub>O<sub>3</sub> catalyst.<sup>87</sup> The dependencies of adsorption and reaction rates upon methyl-group substitution are because of the effects on the electrostatic potential and orbitals rather than steric effects.<sup>87</sup> Massoth et al.<sup>86,87</sup> proposed that the DDO sites consist of a vacancy site with Mo (or Co) exposure and that adjacent HYD sites have S or SH saturated sites, consistent with the results that the DDO route was more inhibited than the HYD route by H<sub>2</sub>S, which could block vacancy site by completion adsorption. Romero et al.<sup>88</sup> proposed that HYD sites could be either the multiple vacancies or the fully sulfided metallic edges (so-called brim sites) located on the basal plane of the MoS<sub>2</sub> slabs, which does not contain vacancies. These are very similar to the proposed site requirements of HDS reaction of thiophene-derived molecules on Mo-based sulfide catalysts.<sup>51</sup> The DDO and HYD reactions of phenols require different sites and different binding phenols on catalyst surfaces. As shown in Figure 6, Romero et al.<sup>88</sup> proposed vertical  $\eta_1$  adsorption of 2-

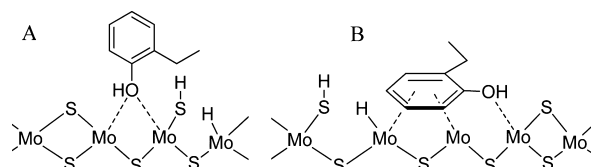


**Figure 6.** Proposed binding modes of 2-ethylphenol on MoS<sub>2</sub> catalyst surface: (A) vertical  $\eta_1$  adsorption of through oxygen and (B) flat  $\eta_5$  adsorption through aromatic ring and oxygen. Redrawn with permission from ref 88. Copyright 2010 Elsevier.

ethylphenol through oxygen on vacancy sites for the DDO route and flat  $\eta_5$  adsorption of 2-ethylphenol through aromatic ring and oxygen for the HYD route on multiple vacancies on MoS<sub>2</sub> surfaces. The flat adsorption of phenol on fully sulfided metallic edges could be expected for the HYD route.

Reports on both vapor-phase and aqueous-phase HDO of phenol on non-sulfided catalysts (e.g., Pd, Pt, and Ni) indicated that the HYD route is favored in the conversion of phenol on these catalysts.<sup>74,75,81,89–97</sup> The vapor-phase hydrogenation of phenol over Pt and Pd supported on alumina was studied by Talukdar et al.<sup>89</sup> in a continuous-flow reactor at 1 MPa and 473–548 K. The selectivity to the HYD products, cyclohexanone and cyclohexanol, was up to 99% at conversion range of 40 to 97%. Pt catalysts favored the production of cyclohexanol while Pd catalysts favored cyclohexanone production. In addition, Pt catalysts showed twice as much conversion as Pd catalysts. Supports also affected gas-phase hydrogenation of phenols on Pd metal. Neri et al.<sup>90</sup> showed that a higher selectivity to cyclohexanone was found on Pd/MgO compared to Pd/Al<sub>2</sub>O<sub>3</sub> at atmospheric pressure and at 393 to 573 K, which was hypothesized to be due to the two different forms of adsorbed phenol at the interface between the support and palladium metal particles. However, contradictory results were reported by Mahata et al.<sup>92</sup> They showed that Pd/Al<sub>2</sub>O<sub>3</sub> was selective for cyclohexanone production whereas Pd/MgO produced cyclohexanone along with cyclohexanol as a minor product for hydrogenation of phenol at 503 K under ambient pressure in a continuous-flow reactor. In addition, Al<sub>2</sub>O<sub>3</sub>-based catalysts showed initial deactivation, while MgO-based catalysts showed significantly improved catalyst life.<sup>92</sup> Wan et al.<sup>98</sup> studied the HDO of cresol using a batch reactor at 573 K and 8.3 MPa. HDO of cresol occurred via both HYD and DDO routes to form toluene and methylcyclohexane when water was used as solvent. The occurrence of the DDO route is because of low H<sub>2</sub> availability by the mass-transfer limitations with water as the solvent. When supercritical heptane was used as solvent and the mass-transfer limitations were eliminated, the major products were methylcyclohexanol and methylcyclohexane via the HYD route. The proposed reaction mechanism, as shown in Figure 7, showed both vertical and coplanar adsorption of cresol on catalyst surface, in which the vertical adsorption via oxygen favored the DDO route to toluene and the coplanar surface adsorption of the aromatic ring favored the HYD route to ring-saturated products. The proposed adsorption modes of cresol on noble metal catalysts resembled those for phenol HDO on MoS<sub>2</sub> surfaces.

Studies on aqueous-phase HDO of phenol using Pd on carbon and Raney Ni catalyst in a batch reactor indicated that these catalysts favor phenol hydrogenation to cyclohexanol at 340 to 423 K.<sup>74,93–96</sup> Phenol does not undergo direct hydrogenolysis (DDO) to benzene on Pd/C at 353 K and 5 MPa of H<sub>2</sub>.<sup>74,95,96</sup> The hydrogenation product of phenol,

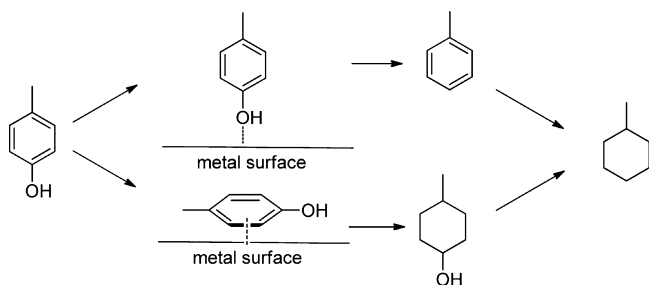


**Figure 7.** Proposed reaction mechanism for HDO of 4-methylphenol on supported Pt, Pd, and Ru metal surface. Redrawn with permission from ref 98. Copyright 2010 Springer.

cyclohexanol, can only undergo oxygen removal by dehydration to cyclohexene catalyzed by acids such as  $\text{H}_3\text{PO}_4$  at  $>473$  K.<sup>74,95,96</sup> As shown in Figure 8, the aqueous-phase dehydration of the intermediate cyclohexanol to cyclohexene is the rate-determining step in the overall phenol HDO reaction on Pd/C and  $\text{H}_3\text{PO}_4$  at 473 K and 5.0 MPa of  $\text{H}_2$ .<sup>74</sup> Consequently, a bifunctional catalyst system, including a metal function and an acid function, was developed to catalyze phenol HDO with a much improved oxygen removal rate under mild conditions. The reaction pathway followed the sequence of phenol hydrogenation on metal surface to form cyclohexanol, which is dehydrated on acidic sites to form cyclohexene. Various aqueous Brønsted acids (e.g.,  $\text{H}_3\text{PO}_4$ ,  $\text{CH}_3\text{COOH}$ , and Nafion solution), together with Pd/C, Ru/C, Rh/C, or metal nanoparticles, were used as bifunctional catalysts for aqueous-phase HDO of phenol to produce cyclohexane via a hydrogenation–dehydration route.<sup>74,95,96,99</sup> In addition, various solid acids were used as either a support or a cocatalyst to achieve bifunctional catalysts for phenol and cresol HDO.<sup>75,81,96,97,100–103</sup> Zhao et al.<sup>75,96</sup> reported that a nearly 100% yield of cycloalkane was achieved for aqueous-phase HDO of phenol at 473 K and 4.0–5.0 MPa of  $\text{H}_2$  using Pd/C or Raney Ni with  $\text{SiO}_2$ -supported Nafion or HZSM-5 as the Brønsted solid acid. Zhao et al.<sup>101</sup> later investigated the kinetics of aqueous phenol HDO on Ni/HZSM-5 catalysts and showed that phenol hydrogenation was the rate-determining step, which was in contrast to the results on Pd/C with  $\text{H}_3\text{PO}_4$  shown above, indicating that the balance of activity and quantity of metal and acid sites was critical for the performance of the catalysts. Foster et al.<sup>103</sup> reported that the increase of number and strength of acid sites on the  $\gamma\text{-Al}_2\text{O}_3$  support, by modification with base or acid treatments, increased the rate of HDO on Pt/ $\gamma\text{-Al}_2\text{O}_3$  at 533 K and 0.05 MPa.

Zhao et al.<sup>97</sup> used a large-pore molecular sieve HBEA-supported Pd catalyst<sup>97</sup> or Pd/C with H/La-BEA<sup>100</sup> for the conversion of phenol and substituted phenols to form desired bicycloalkanes via HDO and hydroalkylation reaction at 473 to 523 K. The proposed mechanism involves the parallel reactions occurring after the hydrogenation of phenol to cyclohexanol: cyclohexanol dehydration to form cyclohexene or addition of cyclohexanol or cyclohexene to phenol by alkylation, both on

Brønsted acid sites. The preference of the two reactions was influenced by variations of solid acid, steric constraints, temperature, metal sites, and metal–reactant ratios. A highly selective aqueous-phase hydroalkylation and deoxygenation of substituted phenols was achieved over an HBEA-supported Pd catalyst (metal–acid ratio: 1:22 mol/mol) for the production of C12–C18 bicycloalkanes with yields up to 80%. Hong et al.<sup>81</sup> used zeolite-supported Pt catalyst for HDO of aqueous phenol in a continuous-flow reactor at 473 to 523 K and 4 MPa of  $\text{H}_2$ . The selectivity of HYD route was more than 98%, and the acid functions of zeolite led to high activity and selectivity to monocyclics and the production of useful bicyclics. Acid function of the bifunctional catalyst apparently could catalyze both the dehydration reaction to accelerate phenol HDO to cyclohexane and the hydroalkylation reaction to produce useful bicycloalkanes.

#### 4.2. HDO of Anisole, Guaiacol, and Phenolic Dimers.

The HDO of anisole was conducted on an  $\text{Al}_2\text{O}_3$  supported CoMo sulfide catalyst at between 473 and 573 K and 1.5 MPa of  $\text{H}_2$  in a continuous-flow reactor.<sup>104</sup> As shown in Figure 9, the

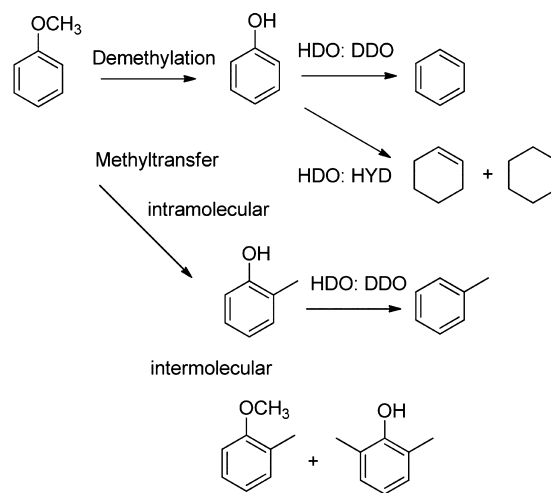


**Figure 9.** Reaction network of HDO of anisole on sulfide CoMo catalyst. Redrawn with permission from ref 104. Copyright 2000 Elsevier.

primary reaction of anisole included demethylation to form methane and phenol and transalkylation to produce methylphenol and dimethylphenol. The further conversion of phenols follows either HYD or DDO routes. A methyl transfer reaction is desirable in the HDO reaction because it prevents the loss of carbon in methoxyl ( $-\text{OCH}_3$ ), one of the major functional groups in lignin-derived phenolics. Li et al.<sup>72</sup> studied the HDO of anisole over silica-supported  $\text{Ni}_2\text{P}$ , MoP, and NiMoP catalysts at 573 K and 1.5 MPa. Only phenol, benzene, and cyclohexane were detected as main products, indicating that the HDO of anisole under these conditions mainly proceeds via demethylation to phenol followed by DDO or HYD routes of phenol to hydrocarbon. HDO activities decreased in the

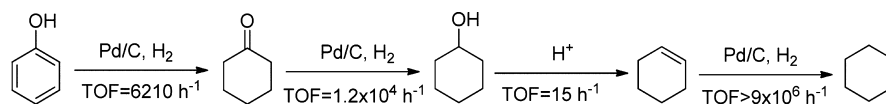


**Figure 8.** Reaction pathway for aqueous-phase HDO of phenol on dual-functional catalysts of Pd/C and  $\text{H}_3\text{PO}_4$  at 473 K. The turnover frequency for each step is also presented. Redrawn with permission from ref 74. Copyright 2010 Elsevier.



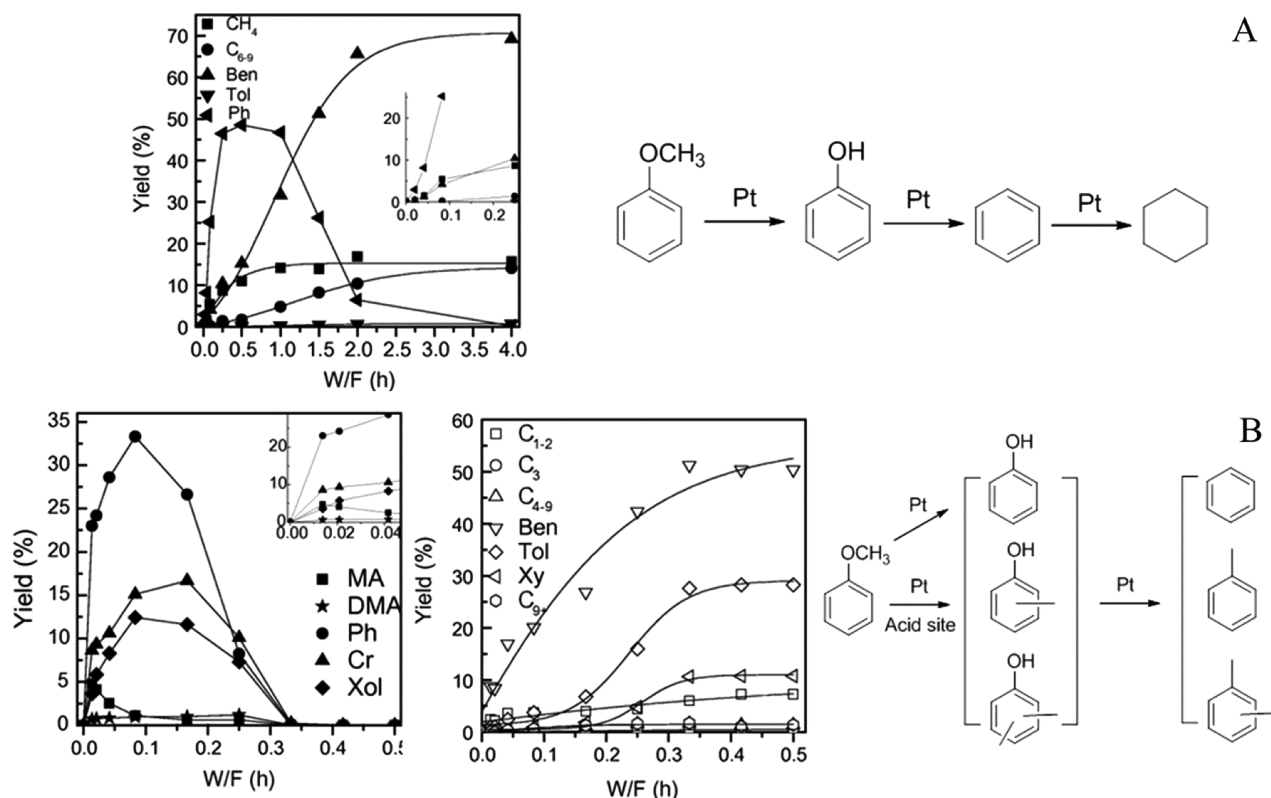


**Figure 10.** Product yield against  $W/F$  (the ratio of catalyst mass to organic feed flow rate) and the corresponding reaction network of HDO of anisole on (A) Pt/SiO<sub>2</sub> and (B) Pt/H-Beta catalyst at 673 K and 0.1 MPa (Ben, benzene; Tol, toluene; Ph, phenol; Xy, xylene isomers; MA, methylanisole; DMA, dimethylanisole isomers; Cr, cresol isomers; Xol, xylol isomers). Redrawn with permission from ref 80. Copyright 2011 Elsevier.

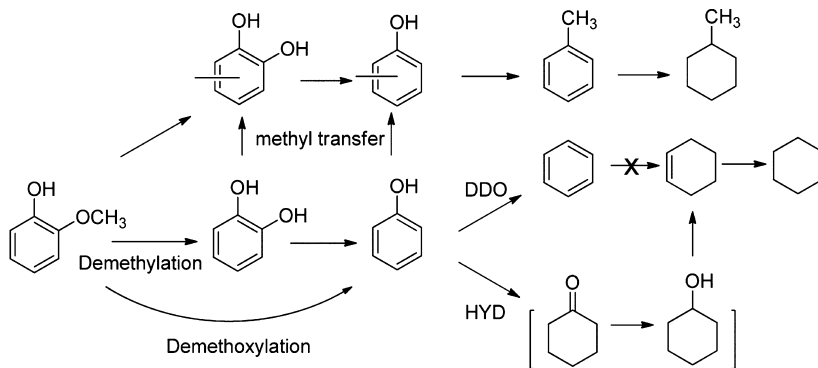


**Figure 11.** Reaction scheme for guaiacol conversion on alumina-supported CoMo sulfide catalyst at 573 K under 4 MPa of H<sub>2</sub>. Redrawn with permission from ref 108. Copyright 2009 Elsevier.

sequence of Ni<sub>2</sub>P/SiO<sub>2</sub> > NiMoP/SiO<sub>2</sub> > MoP/SiO<sub>2</sub>, and the Ni phosphide-containing catalysts showed much higher activities than a conventional NiMo/ $\gamma$ -Al<sub>2</sub>O<sub>3</sub> catalyst.

The HDO of anisole on a Pt/Al<sub>2</sub>O<sub>3</sub> catalyst was conducted by Runnebaum et al.<sup>105</sup> at 573 K and 0.14 MPa of H<sub>2</sub> in a continuous-flow reactor, which showed the major primary reactions of demethylation to phenol, methyl transfer reaction to methyl phenols, and deoxygenation to benzene and methanol. As shown in Figure 10A a study of anisole HDO on a SiO<sub>2</sub>-supported Pt catalyst conducted by Zhu et al.<sup>80</sup> at 673 K and 0.1 MPa of H<sub>2</sub> in a continuous-flow reactor indicated that demethylation of anisole to form phenol and methane was the primary reaction. No direct hydrogenation of anisole or the produced phenol was observed. The decomposed methyl group

did not remain on the surface nor was it transferred to another molecule, rather it was rapidly hydrogenated to form methane. An isomerization catalyst, Pt/H-Beta, was chosen as a bifunctional catalyst to provide acid sites to catalyze the alkyl transfer reaction. As shown in Figure 10B, a significant amount of toluene, xylenes, and C<sub>9</sub> isomers were produced at high  $W/F$  (the ratio of catalyst mass to organic feed flow rate), indicating that acidic function (H-Beta) catalyzed the methyl transfer reaction (transalkylation) from methoxyl to the aromatic ring. Bifunctional catalysts showed higher rates for the formation of aromatics, lower hydrogen consumption, and a significant reduction in carbon losses compared to catalysts with only a metal function.<sup>80</sup> In addition, bifunctional Pt/H-Beta exhibited lower rate of deactivation and less coke deposition.<sup>80</sup> Zhao et

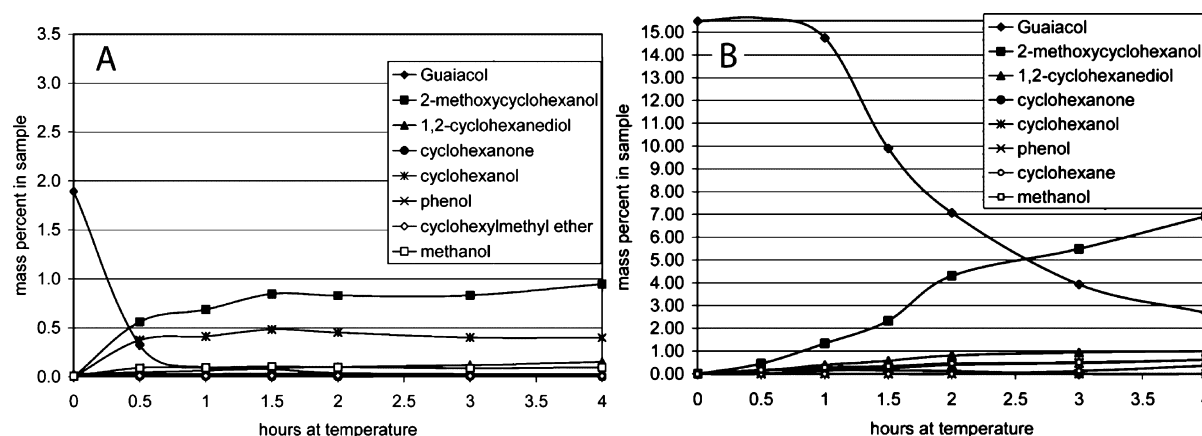


**Figure 12.** Reactant and product distribution of guaiacol HDO at 4.2 MPa of  $H_2$  on (A) Ru/C at 473 K and (B) Pd/C at 523 K. Adapted with permission from ref 77. Copyright 2009 American Chemical Society.

al.<sup>74</sup> tested the HDO of anisole at 423 K and 5 MPa of  $H_2$  on the bifunctional catalyst system consisting of Pd/C with  $H_3PO_4$  in a batch reactor. The two primary reactions were found to be hydrogenation of anisole to methoxycyclohexane by metal function and hydrolysis of anisole to phenol by acid function. The appearance of hydrogenation of anisole as the primary reaction was because of the high pressure of  $H_2$  used.

Guaiacol and substituted guaiacols have attracted much attention among studies of HDO of bio-oil model compounds because they have the representative functional groups in phenolics and are relatively stable under the temperature of pyrolysis.<sup>42</sup> Early studies using mainly supported Mo-based sulfide catalysts showed that the basic reaction scheme of guaiacol HDO involves a consecutive pathway from guaiacol to catechol by demethylation and then to phenol by deoxygenation.<sup>42,76,106,107</sup> However, some recent studies also suggested the additional routes including direct demethoxylation of guaiacol to phenol and methyl transfer reaction to methylcatechols during HDO of guaiacol on Mo-based sulfide catalysts.<sup>71,78,108,109</sup> Figure 11 shows a general reaction scheme reported by Bui et al.<sup>108</sup> for guaiacol conversion on alumina-supported CoMo sulfide catalyst at 573 K under 4 MPa of  $H_2$ . In addition, heavier products (coke precursors) might be formed during the reaction, especially with the acidic catalytic systems.

Zhao et al.<sup>73</sup> conducted HDO of guaiacol on 573 K and atmospheric pressure on  $SiO_2$ -supported transition metal phosphides including  $Ni_2P$ ,  $Fe_2P$ , MoP,  $Co_2P$ , and WP in a continuous-flow reactor. The major products for the most active phosphides were benzene and phenol (and a small amount of anisole), with formation of reaction intermediates (e.g., catechol and cresol) at short contact times. This indicates that HDO of guaiacol on metal phosphide follows similar routes on metal sulfides including demethylation–deoxygenation, demethoxylation, and methyl transfer reaction. The observation of anisole as a product also indicated that the direct deoxygenation of guaiacol to remove OH group occurs as a new route of guaiacol HDO. The activity for HDO of guaiacol follows the order  $Ni_2P > Co_2P > Fe_2P$ , WP, MoP. The 8.6 wt %  $Ni_2P/SiO_2$  catalysts are less active than a commercial 5 wt % Pd/ $Al_2O_3$  catalyst, but much more active than a commercial sulfide CoMo/ $Al_2O_3$ .

Elliott and Hart<sup>77</sup> reported on HDO of guaiacol on carbon-supported Ru and Pd catalysts at 423 to 523 K and 4.0 MPa of hydrogen in a batch reactor. As shown in Figure 12,

hydrogenated guaiacol, 2-methoxycyclohexanol, is the major product, indicating a completely different reaction route than on Mo-based sulfide catalysts. The hydrogenation route using the Ru catalyst proceeded via methoxycyclohexanol to cyclohexanediols at low temperatures and continued to form cyclohexanol at higher temperatures (Figure 12A). At 523 K and above, gasification reactions dominated. The Pd catalyst led first to methoxycyclohexanone at 423 K and then methoxycyclohexanol at 473 K with some cyclohexanediol. At 523 K, as shown in Figure 12B, the product slate was shifted toward cyclohexanol and cyclohexane (without gasification), but at 573 K, the product slate was shifted strongly to cyclohexane with a large amount of methanol byproduct. Gutierrez et al.<sup>110</sup> studied HDO of guaiacol on  $ZrO_2$ -supported mono- and bimetallic noble metal (i.e., Rh, Pd, Pt) catalysts using a batch reactor at 373 and 573 K and 8.0 MPa of  $H_2$ . At low temperature (373 K), hydrogenated oxygen-containing compounds were produced as major products and methyl transfer reaction occurred. The performance of the noble metal catalysts, especially the Rh-containing catalysts, was similar to or better than that of the conventional sulfided CoMo/ $Al_2O_3$  catalyst. Bykova et al.<sup>111</sup> studied the guaiacol HDO on Ni-based sol–gel catalysts at 593 K and 17 MPa in a batch reactor. Major products were hydrogenated intermediates and cyclohexane, indicating a preference of hydrogenation route.

Lin et al.<sup>71</sup> demonstrated the different reaction routes involved in HDO of guaiacol between noble metal and Mo-based sulfide catalyst by comparing reactions on Rh-based catalysts and sulfide CoMo and NiMo catalysts at 573 to 673 K and 5.0 MPa of  $H_2$  in a batch reactor. Sulfided CoMo and NiMo produced methoxybenzene, methylphenol, phenol, benzene, cyclohexene, and cyclohexane, consistent with their proposed reaction network for guaiacol HDO on sulfide catalysts, which assembles the general reaction scheme on sulfide catalyst as discussed above. However, Rh-based catalysts produced 2-methoxycyclohexanol, 2-methoxycyclohexanone, 1-methoxycyclohexane, cyclohexanol, cyclohexanone, and cyclohexane, suggesting that the mechanism of guaiacol HDO by Rh-based catalysts involved two consecutive steps: hydrogenation of the guaiacol benzene ring, followed by demethoxylation and dehydroxylation of oxygenates, as shown in Figure 13. They concluded that the Rh-based catalyst exhibited the best HDO activity with the preference to saturate benzene rings, while conventional sulfided CoMo and NiMo catalysts

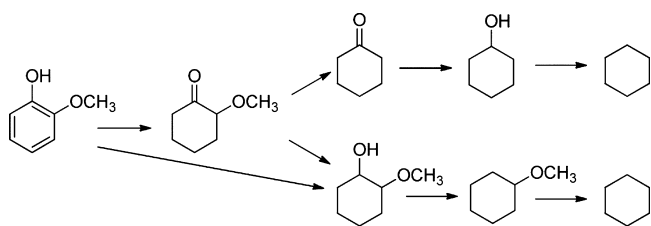


**Figure 13.** Reaction network of guaiacol HDO by Rh-based catalysts. Redrawn with permission from ref 71. Copyright 2011 American Chemical Society.

were much less active compared to noble metals on both hydrogenation and deoxygenation reaction.

Zhao et al.<sup>74,95</sup> tested the aqueous-phase HDO of guaiacol on a bifunctional catalyst system (Pd/C and H<sub>3</sub>PO<sub>4</sub>) at 423 K and 5 MPa of H<sub>2</sub> in a batch reactor. The primary product was the intermediately hydrogenated 2-methoxycyclohexanone (selectivity of 100% at  $t = 0$ ) by the metal-catalyzed hydrogenation of the aromatic ring. As shown in Figure 14, the proposed reaction

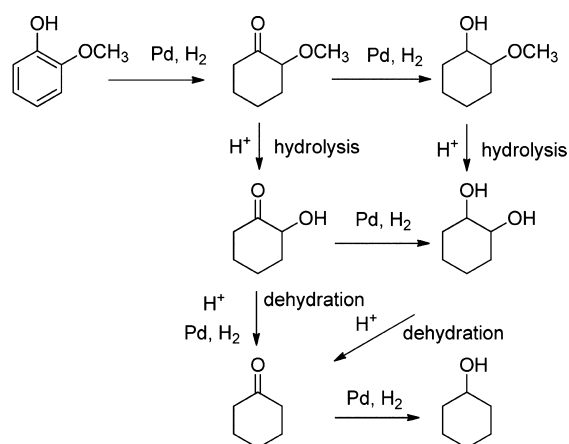


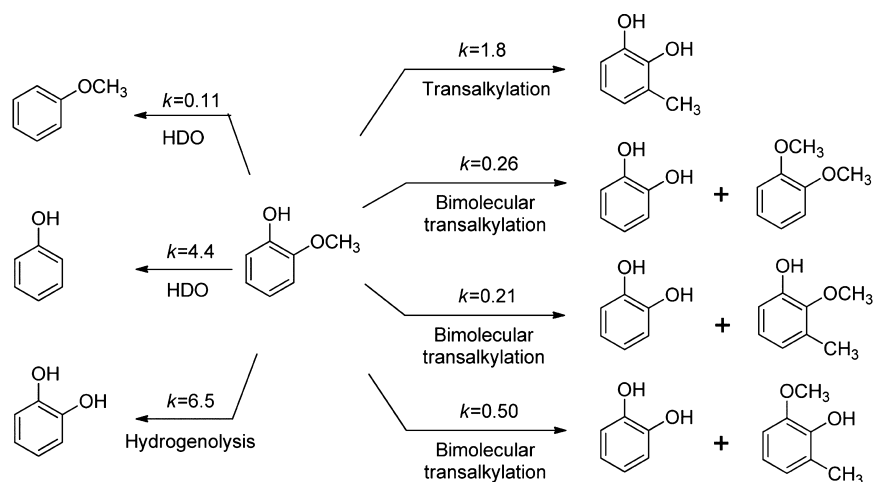
**Figure 14.** Proposed reaction pathway of aqueous-phase HDO of guaiacol on Pd/C with H<sub>3</sub>PO<sub>4</sub>-H<sub>2</sub>O at 423 K and 5 MPa of H<sub>2</sub>. Redrawn with permission from ref 74. Copyright 2011 Elsevier.

pathway includes the acid-catalyzed hydrolysis of the methyl group of hydrogenated intermediate to form 1,2-cyclo-

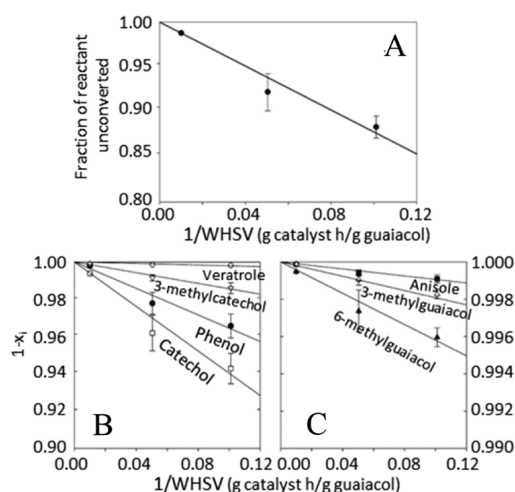
hexanediol, followed by acid-catalyzed dehydration to cyclohexenol. Another bifunctional catalyst system (Pd/C and HZSM-5) showed 100% conversion of guaiacol to cyclohexane at 473 K and 5 MPa of H<sub>2</sub> in a batch reactor.<sup>75</sup>

In addition, HDO of guaiacol was investigated at a low H<sub>2</sub> pressure (<0.1 MPa) and a high temperature (573 to 673 K), which matched the conditions of catalysis process for upgrading pyrolysis vapor in catalytic fast pyrolysis. Under these conditions, hydrogenation of the aromatic ring of guaiacol was not preferred, as reported by Nimmanwudipong et al.<sup>112–114</sup> and Runnebaum et al.<sup>115</sup> using Pt/ $\gamma$ -Al<sub>2</sub>O<sub>3</sub> and Pd/MgO with a continuous-flow reactor at 573 K and 0.14 MPa and by Olcese et al.<sup>116</sup> using Fe/SiO<sub>2</sub> with a continuous-flow reactor at 623 to 723 K and 0.02 to 0.09 MPa. As shown in Figure 15, the main primary products of guaiacol HDO on Pt/ $\gamma$ -Al<sub>2</sub>O<sub>3</sub> were catechol, phenol, and 3-methylcatechol, which were from either C–O hydrogenolysis or methyl transfer reaction of guaiacol.<sup>113</sup> The lack of hydrogenation of aromatic ring is probably due to the relatively low H<sub>2</sub> pressure (0.14 MPa) used compared to the above studies on noble metal catalysts (4.0 to 8.0 MPa of H<sub>2</sub>). Kinetic analysis has shown that a semilogarithmic plot of the fraction of guaiacol unconverted as a function of inverse space velocity was nearly linear, indicating that the overall guaiacol conversion was well-represented by first-order kinetics over the conversion range (Figure 16A).<sup>113</sup> The conversion to individual primary products is also well-represented by first-order kinetics over the ranges of conversion studied, as shown in Figures 16B and 16C. Therefore, the pseudo-first-order rate constants for the disappearance of guaiacol and for the formation of the primary products were calculated and are given in Figure 15. Pt/MgO catalyst was more stable than Pt/ $\gamma$ -Al<sub>2</sub>O<sub>3</sub> because of the relative lack of coke formation, indicating an advantage of using basic supports for HDO catalysts.<sup>114</sup> In addition, Fe/SiO<sub>2</sub> was an active and selective catalyst for the conversion of guaiacol to aromatics at 673 K.<sup>116</sup>

A significant amount of phenolic dimers was formed during the thermal deconstruction of lignin, which represents an important fraction in bio-oil. Aqueous-phase HDO of phenolic dimers was conducted by Zhao et al.<sup>75,82</sup> on bifunctional Pd/C with HZSM-5 catalyst and Ni/ZSM-5 at 473 to 523 K and 5.0 MPa in a batch reactor. The  $\beta$ -O-4 and  $\alpha$ -O-4 dimer (alkyl-



**Figure 15.** Reaction network of guaiacol on Pt/Al<sub>2</sub>O<sub>3</sub> at 573 K and 0.14 MPa of H<sub>2</sub>. Pseudo-first-order rate constants for the primary reactions are shown in units of L (g of catalyst)<sup>-1</sup> h<sup>-1</sup>. Redrawn with permission from ref 113. Copyright 2011 American Chemical Society.

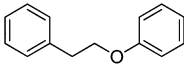
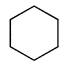
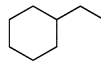
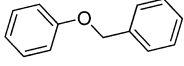
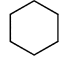
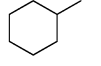
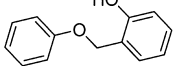
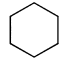
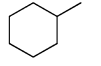
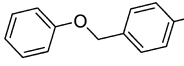
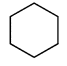
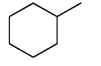
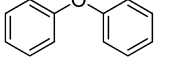
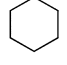
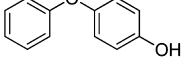
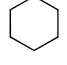
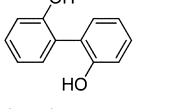
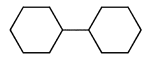
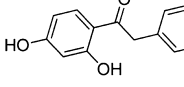
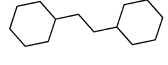
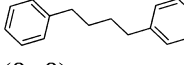
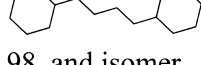


**Figure 16.** Demonstration of first-order kinetics of (A) overall conversion and (B and C) conversion to each primary product of guaiacol HDO on Pt/γ-Al<sub>2</sub>O<sub>3</sub> at 573 K and 0.14 MPa of H<sub>2</sub>. The term  $x_i$  represents the conversion to product  $i$ . Conversion was varied by changing the catalyst mass. Redrawn with permission from ref 113. Copyright 2011 American Chemical Society.

aryl ether) was quantitatively converted to phenol and alkylated aromatic at a low conversion and to cyclohexane and alkylated cyclohexane as final products (Table 7).<sup>75</sup> The mechanism for the HDO of β-O-4 and α-O-4 model compounds started with the metal-catalyzed hydrogenolysis of the ether to phenol and arenes, followed by the hydrogenation–dehydration of the phenols and the hydrogenation of the arenes on the metal/acid bifunctional catalyst. The 4-O-5 dimers were quantitatively converted to cyclohexane; however, they remained unchanged using HZSM-5 only, indicating that both metal and HZSM-5 are essential for the cleavage of the aryl–aryl ether bond. The C–C linkages in 5-5, β-1, and β-β were preserved, whereas the substituted hydroxyl and ketone groups were selectively removed, leading to C12, C14, and C16 bicycloalkanes, respectively. Strassberger et al.<sup>117</sup> studied the HDO of β-O-4 lignin-type dimers on supported Cu catalysts at 423 K and 2.5 MPa in a batch reactor, which showed both β-O-4 cleavage products (phenolics) and HDO products (aromatics).

**4.3. HDO of Furans and Furfurals.** HDO of furans, including furan, methylfuran, dimethylfuran, benzofuran, and dibenzofuran, have attracted the most attention among the studies of the HDO of fuel oil using supported Mo-based sulfide catalysts. The products from the HDO of furan, methylfuran, and dimethylfuran are mainly hydrocarbons including isomers of alkene, alkane, and small amounts of alkenadiene.<sup>42</sup> Alkene and alkane arose from hydrogenated furans (HYD route) and/or hydrogenation of alkenadiene that formed from direct deoxygenation of furans (DDO route). Furan can be completely hydrogenated to tetrahydrofuran under typical hydroprocessing conditions, and the HDO of tetrahydrofuran was much faster than that of the furan, indicating that tetrahydrofuran is an important intermediate during furan HDO.<sup>118,119</sup> Detailed studies on the vapor-phase HDO of benzofuran on sulfide CoMo catalyst at 6.5 MPa of H<sub>2</sub> and 533 to 583 K have shown that the reaction followed the sequences of hydrogenation to 2,3-dihydrobenzofuran, C–O cleavage to *o*-ethylphenol, second C–O cleavage to ethylbenzene, and hydrogenation to ethylcyclohexene and ethylcyclohexane. C–C bond hydrogenolysis occurred to produce small amounts of

**Table 7.** Aqueous-Phase HDO of Phenolic Dimers on Pd/C and HZSM-5 Catalysts at 473 K and 5.0 MPa of H<sub>2</sub><sup>75,a</sup>

Phenolic Dimers	Product and Selectivity (C%)	
 (β-O-4)		
	46	54
 (α-O-4)		
	48	52
 (α-O-4)		
	48	52
 (α-O-4)		
	44	56
 (4-O-5)		
	100	
 (4-O-5)		
	100	
 (5-5)		
	85, and isomer	
 (β-1)		
	95, and isomer	
 (β-β)		
	98, and isomer	

<sup>a</sup>The conversion is 100% for all feeds.

phenol, toluene, and benzene. A study by Bunch et al.<sup>120</sup> on vapor-phase HDO of benzofuran on reduced NiMo catalyst at 393 to 633 K and 2.0 to 5.0 MPa found the further hydrogenation of 2,3-dihydrobenzofuran to octahydrobenzofuran. HDO of benzofuran appeared to occur exclusively via hydrogenation (HYD) route. However, it is possible that hydrogenation of styrene, the primary product of direct deoxygenation (DDO), is fast and therefore is not detected in the products. HDO of dibenzofuran occurred via both DDO route to biphenyl and HYD route to hexahydrodibenzofuran on sulfide NiMo and CoMo catalysts.<sup>121</sup> Hydrogenation of biphenyl and deoxygenation of hexahydrodibenzofuran occurred subsequently. The formed hydrocarbons were further converted to the single-ring products.

Few studies have investigated the HDO of furan on noble metal catalysts. Furan hydrogenation was carried out by Kliever et al.<sup>122</sup> over Pt nanoparticles with 10 Torr of furan and 100 Torr of H<sub>2</sub> at 353 to 413 K. Dihydrofuran, tetrahydrofuran,

butanol, and propylene were all detectable products. As shown in Figure 17A, the conversion of butanol to propylene increases

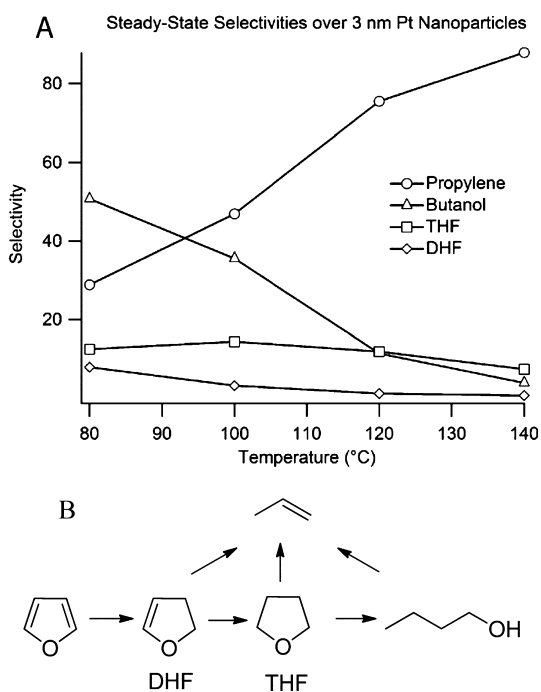
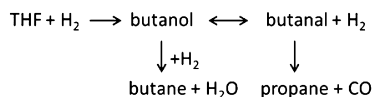


**Figure 17.** HDO of furan over Pt nanoparticles. (A) product selectivity as a function of reaction temperature over 3 nm Pt nanoparticles and (B) reaction network. Redrawn with permission from ref 122. Copyright 2010 American Chemical Society.

as the temperature increases from 353 to 413 K. A reaction network was proposed, as shown in Figure 17B. Spectroscopy analysis suggested that the furan ring adsorbed on Pt surfaces via flat adsorption and tetrahydrofuran and oxametallacycle intermediate bound on metal surfaces vertically under reaction conditions. Study of HDO of tetrahydrofuran on supported Pt catalysts at 423 to 573 K by Kreuzer and Kramer<sup>123</sup> showed that the primary reaction was C–O bond cleavage to open the five-membered ring. The primary product butanol underwent a second C–O bond cleavage to form butane and H<sub>2</sub>O or C–C bond cleavage via butanol to form propane and CO.



Liu et al.<sup>124</sup> studied the HDO of benzofuran over silica–alumina-supported Pt, Pd, and alloyed Pt–Pd catalysts at 553 K and 3.0 MPa. Only the hydrogenation–deoxygenation (HYD) route was found for the conversion of benzofuran, which was first hydrogenated to 2,3-dihydrobenzofuran and then to

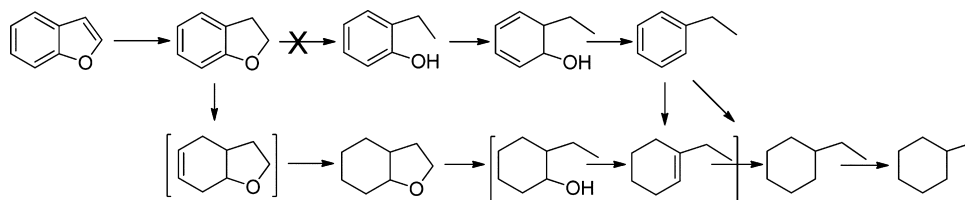


**Figure 18.** Reaction network for HDO of benzofuran over silica–alumina-supported Pt, Pd, and Pt–Pd catalysts at 553 K and 3.0 MPa. Redrawn with permission from ref 124. Copyright 2012 American Chemical Society.

octahydrobenzofuran, followed by deoxygenation to cyclohexanes, as shown in Figure 18. Bimetallic Pt–Pd catalysts showed higher activities in hydrogenation and oxygen removal than their monometallic counterparts did. Bowker et al.<sup>125</sup> reported that the Ru phosphide catalysts (Ru<sub>2</sub>P/SiO<sub>2</sub> and RuP/SiO<sub>2</sub>) exhibited furan HDO activities similar to or higher than a Ru/SiO<sub>2</sub> catalyst, and the phosphide catalysts favored C4 hydrocarbon products (butene and butane, C–O cleavage) while the Ru metal catalyst produced primarily C3 hydrocarbons (propene and propane, C–C cleavage). These Ru-based catalysts were much more active than a commercial CoMo sulfide catalyst.

Furfural is another important component commonly found in bio-oil. Due to its high reactivity, this compound needs to be catalytically hydrogenated or hydrodeoxygenated to improve bio-oil stability. Early studies on furfural have focused on the hydrogenation of furfural to furfuryl alcohol, 2-methylfuran, and tetrahydrofuran using supported Cu,<sup>126</sup> Pt,<sup>127</sup> Ni–B alloy,<sup>128</sup> and Cu–Cr<sup>129</sup> catalysts. Figure 19 shows a reaction pathway for

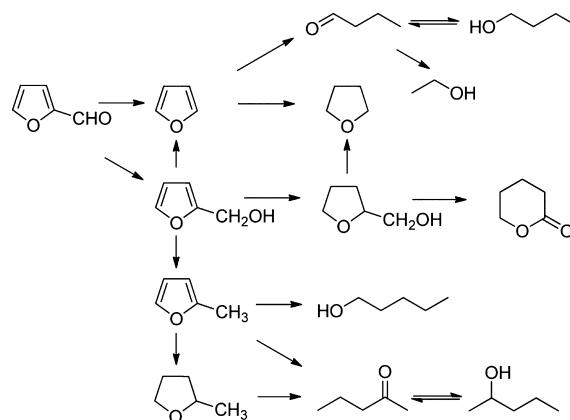


**Figure 19.** Reaction pathway proposed for furfural HDO (VL: valerolactone). Redrawn with permission from ref 129. Copyright 2006 Elsevier.

furfural hydrogenation proposed by Zheng et al.<sup>129</sup> for gas-phase reaction at 543 K and atmospheric pressure on Cu/Zn/Al/Ca/Na catalysts. Primary reaction of furfural involves hydrogenation of C=O to furfural alcohol and hydrogenolysis of C–C bond to furan. Furan reacts further via HYD or DDO to tetrahydrofuran or butanal and butanol, respectively, as discussed above. Furfural alcohol produces 2-methylfuran via C–O bond cleavage, furan via C–C bond cleavage, and tetrahydrofurfuryl alcohol via hydrogenation.

Elliott and Hart<sup>77</sup> studied HDO of furfural on carbon-supported Ru and Pd catalysts at 423 to 523 K and 4.0 MPa of hydrogen in a batch reactor. As shown in Figure 20A, at 473 K, the major product of the HDO of furfural on Ru catalyst was

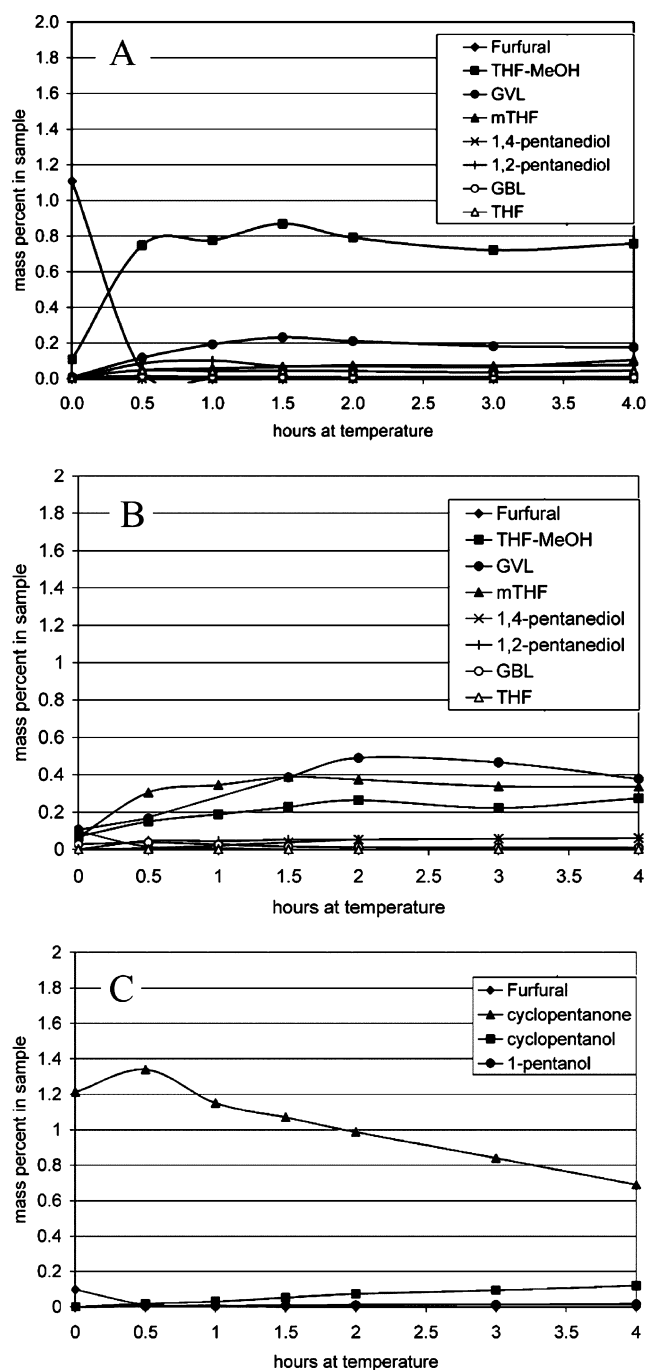


**Figure 20.** (A) Cyclic ether pathway product distribution of furfural conversion over Ru/C at 473 K. (B) Cyclic ether pathway product distribution of furfural conversion over Pd/C at 473 K. (C) Cyclic ketone pathway product distribution from furfural conversion over Pd/C at 473 K. (GVL,  $\gamma$ -valerolactone; GBL,  $\gamma$ -butyrolactone; THF, tetrahydrofuran.) Adapted with permission from ref 77. Copyright 2011 American Chemical Society.

tetrahydrofurfuryl alcohol (THF-MeOH), a completely hydrogenated furfural. Other prominent products included  $\gamma$ -valerolactone (GVL), methyltetrahydrofuran (mTHF), pentaediol, and cyclopentanol. At higher temperatures (i.e., 523 and 573 K), tetrahydrofurfuryl alcohol quickly converted to methyltetrahydrofuran and tetrahydrofuran. As shown in Figures 20B and 20C, at 473 K and on Pd catalyst, major products were cyclopentanone and cyclopentanol. Methyl-

tetrahydrofuran, tetrahydrofurfuryl alcohol, and  $\gamma$ -valerolactone were other prominent products. At higher temperature, methyltetrahydrofuran,  $\gamma$ -valerolactone, and pentanol were the major products at the end of the test. Elliott and Hart concluded that a route from furfural to cyclopentanone and pentanols was an important mechanistic route. At low temperatures, furfural hydrogenation to tetrahydrofurfuryl alcohol appeared to be the primary route for both Ru and Pd catalysts. At 523 K and above, the pathway through  $\gamma$ -valerolactone to 1,4-pentenediol and methyltetrahydrofuran was more important. These authors also performed a single uncatalyzed test at 523 K and observed a solid, polymeric material formed from furfural, indicating that polymerization and even charring of furfural might occur simultaneously during HDO reaction.

Sitthisa et al.<sup>130–132</sup> studied the HDO of furfural on SiO<sub>2</sub>-supported Pd, Cu, Ni, and Pd–Cu catalysts at 503 to 563 K and 0.1 MPa of H<sub>2</sub> in a continuous-flow reactor. Table 8 compares

**Table 8.** Activity and Product Distribution of HDO of Furfural over SiO<sub>2</sub>-Supported Cu, Pd, and Ni Catalysts at 573 K and 0.1 MPa<sup>131</sup>

	10% Cu/ SiO <sub>2</sub>	1% Pd/ SiO <sub>2</sub>	5% Ni/ SiO <sub>2</sub>
TOF (s <sup>-1</sup> )	1.3	265.8	76.5
conversion (%)	69	69	72
hydrogenation (%)			
furfuryl alcohol	98	14	25
2-methylfuran	2		3
tetrahydrofurfuryl alcohol		5	4
decarbonylation (%)			
furan		60	43
tetrahydrofuran		20	
ring-opening (%)			
butanal			12
butanol			3
butane			10

the activity and product selectivities on the three monometallic catalysts. The conversion of furfural on Cu/SiO<sub>2</sub> yields mainly furfuryl alcohol from hydrogenation of the carbonyl, with only small amounts of 2-methylfuran, obtained from a subsequent cleavage of the C–O bond in furfuryl alcohol. A Langmuir–Hinshelwood model was used to fit the kinetic data and provide the parameters of physical significance. The rate constant for the hydrogenation of furfural was significantly higher than that for HDO of furfuryl alcohol to produce 2-methylfuran. The heat of adsorption for furfural (12.3 kcal/mol) was similar to that of adsorption of water (12.4 kcal/mol), but higher than those for furfuryl alcohol (6.9 kcal/mol) and 2-methylfuran (3.7 kcal/mol). On the Pd catalyst, furfural conversion was described as two parallel routes: (i) decarbonylation to furan that subsequently hydrogenates to tetrahydrofuran and (ii) hydrogenation to furfuryl alcohol that subsequently hydrogenates to tetrahydrofurfuryl alcohol, as shown in Figure 21 for conversion and product distribution as a function of *W/F* and the corresponding reaction network. Decarbonylation was the dominant reaction even at low *W/F*. The proposed reaction mechanism (see Figure 21B) includes two parallel reactions requiring different intermediates. The preferential formation of an acyl intermediate at higher temperatures, which can readily decompose into CO and hydrocarbons, led to a higher

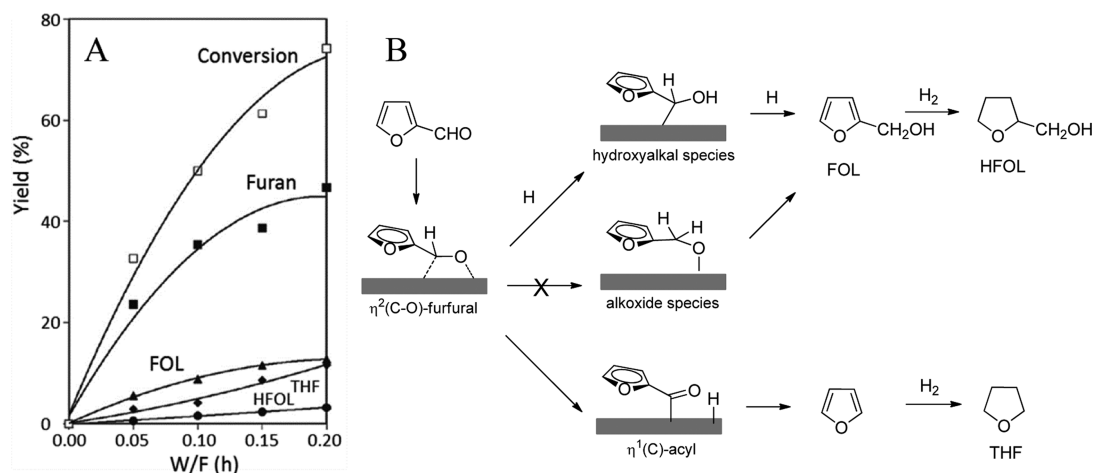


**Figure 21.** Conversion and product distribution (A) from furfural over 0.5% Pd/SiO<sub>2</sub> as a function of W/F at 503 K and 0.1 MPa of H<sub>2</sub> and proposed reaction mechanism (B). (THF, tetrahydrofuran; FOL, furfuryl alcohol; HFOL, tetrahydrofurfuryl alcohol.) Redrawn with permission from ref 132. Copyright 2011 Elsevier.

decarbonylation/hydrogenation ratio. The Pd–Cu alloys, with a lower extent of electron back-donation to the  $\pi^*$  system of the aldehydes, had less preference of formation of acyl intermediates of furfural. Therefore, the decarbonylation rate was reduced on Pd–Cu catalysts, but the hydrogenation rate was increased. The Ni catalyst had a product distribution similar to that of the Pd catalyst. Furan was not as abundant because it further reacted to form ring-opening products due to the interaction of the ring with the surface, which was even stronger than on the Pd catalyst. Zhang et al.<sup>133</sup> conducted a study on the furfural decarbonylation reaction on K-doped Pd/Al<sub>2</sub>O<sub>3</sub> at 453 to 533 K and ambient pressure in a continuous-flow reactor. The doping of K not only promoted the furfural decarbonylation but also suppressed the hydrogenation side reaction.

Zhao et al.<sup>82</sup> studied HDO of furfural and methylfurfural in water on a Ni/HZSM-5 catalyst at 523 K and 5 MPa of H<sub>2</sub> in a batch reactor. Two parallel reactions, intermolecular dehydration of furfural to tetrahydropyran and HDO of furfural to pentane, competed to ultimately produce 64% pentane and 36% tetrahydropyran. The HDO of furfural occurred by hydrogenation of the furan ring, followed by hydrolysis of the C5 ring, and subsequent alcohol dehydration/hydrogenation to form the straight-chain alkane.

**4.4. HDO of Carboxylic Acids.** Carboxylic acids, such as acetic acid, formic acid, and propanoic acid, are found in large amounts in bio-oils and contribute to the acidic and corrosive nature of bio-oil. Therefore, conversion of carboxylic acid during hydrotreating of bio-oil is critical to produce suitable transportation fuels. Early studies on acetic acid conversion have focused on the hydrogenation of acetic acid to acetaldehyde using oxide catalysts (e.g., titania, iron oxide, tin oxide, chromium oxide).<sup>134–138</sup> The addition of Pt to the catalyst enhanced selectivity and activity.<sup>134</sup> Detailed studies on reaction mechanism and kinetics showed that the reduction of acetic acid on oxide-supported Pt catalysts started via a reaction between adsorbed H atoms from the Pt surface and an acyl species on oxide. This pathway was the major route for the production of acetaldehyde, which could be further hydrogenated to ethanol.<sup>138</sup> Pt was used as active sites to activate hydrogen.

Reaction on pure Pt was studied by testing acetic acid conversion on Pt supported on SiO<sub>2</sub>, an inert support, via a temperature-program reaction at 0.12 MPa of H<sub>2</sub> and from 293 to 723 K. Acetic acid was converted at ~593 K, and the main reaction products were methane, water, CO, and CO<sub>2</sub>, obtained from the total decomposition of acetic acid.<sup>134</sup> Gursahani et al.<sup>139</sup> studied reaction pathways for the catalytic conversions of acetic acid over a Pt/SiO<sub>2</sub> catalyst at temperatures from 500 to 600 K and showed that the stoichiometric reaction created an equimolar mixture of CO and CH<sub>4</sub>: CH<sub>3</sub>COOH + H<sub>2</sub> → CH<sub>4</sub> + CO + H<sub>2</sub>O. A small amount of CO<sub>2</sub>, a decarboxylation product of acetic acid, was observed at temperatures >673 K.

Elliott and Hart studied HDO of acetic acid on Pd/C and Ru/C catalysts at 473 to 573 K and 4.0 MPa of hydrogen in a batch reactor.<sup>77</sup> Acetic acid was hydrogenated to ethanol with moderate yields on Pd/C at 573 K, with a small amount of ethyl acetate as a secondary condensation product. Acetic acid was not effectively hydrogenated to ethanol on Ru catalyst, rather it decomposed to methane and carbon dioxide at temperatures where there was significant activity. Olcay et al.<sup>140</sup> studied aqueous-phase hydrogenation of acetic acid over transition metal catalysts, including carbon-supported Ru, Rh, Pt, Ir, and Pd, Raney Ni, and Raney Cu at 5.17 MPa of H<sub>2</sub> and at 383 to 683 K. The turnover rate of acetic acid conversion decrease in the order Ru > Rh ≈ Pt > Pd ≈ Ir > Ni > Cu. The Ru/C catalyst showed 70 to 80% selectivity for ethanol, the hydrogenation product, at temperatures below 448 K and 83% selectivity for methane, the decomposition product, at 498 K. Pallassana and Neurock<sup>141</sup> carried out density functional theory calculations to examine alternative mechanisms for the hydrogenolysis of acetic acid to ethanol over Pd. The overall reaction energy results indicated that the most favorable path for acetic acid hydrogenolysis involved the formation of an acetyl intermediate, followed by its hydrogenation to acetaldehyde. The acetaldehyde was subsequently hydrogenated to form ethanol.

Gas-phase HDO of propionic acid on Pd/SiO<sub>2</sub> and Pt/SiO<sub>2</sub> catalysts at 523 to 673 K under atmospheric pressure led to almost 100% selectivity to ethane, suggesting that hydrogenolysis of C–C bond played an essential role.<sup>142</sup> However, Cu/SiO<sub>2</sub> catalyst primarily converted propionic acid to propanal and 1-propanol by C=O hydrogenation. Turnover

rates of propionic acid conversion followed the order Pd > Pt > Cu. Improved activities were observed when bulk acidic salt ( $\text{Cs}_{2.5}\text{H}_{0.5}\text{PW}_{12}\text{O}_{40}$ , CsPW) was used as a support to achieve metal–acid bifunctional catalysis. Hydrogenation of propionic acid was observed on Pd/CsPW and Pt/CsPW catalysts at low temperature, in contrast with  $\text{SiO}_2$ -supported catalysts, suggesting that propionic acid hydrogenation took place on the CsPW polyoxometalate, possibly by a Mars–van Krevelen mechanism. Aqueous-phase HDO of propanoic acid over Ru/ZrO<sub>2</sub> catalysts at 463 K and 6.4 MPa showed that the C–C bond cleavage to methane and ethane was the dominant reaction compared to C=O hydrogenation to propanol and propane at high temperatures,<sup>143</sup> indicating a preferential formation of propanoyl intermediate, which decomposed into CO and hydrocarbons. Addition of Mo to Ru catalyst inhibited the C–C bond cleavage reaction of propanoic acid; however, the conversion decreased due to the formation Ru–MoO<sub>x</sub> and the stability and variety of propanoyl intermediate species on the Ru–Mo surface.

**4.5. HDO of Other Oxygenates.** Wildschut et al.<sup>144</sup> conducted HDO of D-glucose, D-cellobiose, and D-sorbitol, the representative model components for the carbohydrate fraction in bio-oil at 523 K and 10 MPa of H<sub>2</sub> using Ru on carbon catalysts in water. Two parallel reaction routes were reported: a hydrogenation route leading to smaller polyols and gaseous hydrocarbons (e.g., methane and ethane) and a thermal noncatalyzed route leading to insoluble humins (char). The authors suggested that at least part of the gas-phase components and solids formed upon hydrotreating of bio-oils arose from the carbohydrate fraction in the oil.

Sitthisa et al.<sup>132</sup> studied gas-phase HDO of 2-methylpentanal on  $\text{SiO}_2$ -supported Pd and Pd–Cu catalysts at 398 K and 0.1 MPa of H<sub>2</sub>. On the Pd catalyst, the primary reactions of 2-methylpentanal were decarbonylation to pentane and hydrogenation to 2-methylpentanol. Further, etherification occurred between 2-methylpentanal and formed 2-methylpentanol to produce ether. The reaction network is shown in Figure 22. Upon addition of Cu, both the overall activity and the decarbonylation selectivity decreased and the selectivity to hydrogenation and etherification increased.

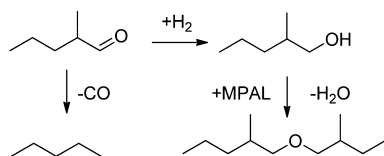


**Figure 22.** Reaction network of the HDO of 2-methylpentanal (MPAL). Redrawn with permission from ref 132. Copyright 2011 Elsevier.

Li and Huber<sup>145</sup> investigated the HDO of 1- and 2-butanol, intermediates of HDO of sorbitol, on Pt/ $\text{SiO}_2$ – $\text{Al}_2\text{O}_3$  at 518 K and 2.93 MPa in a continuous-flow reactor. Butane, propane, and CO<sub>2</sub> were the final products for 1-butanol, whereas butane was the only product for 2-butanol. C–C bond cleavage was more preferable than C–O bond cleavage for 1-butanol under the reaction conditions. As shown in Figure 23, 1-butanol can go through a continuous dehydrogenation and decarbonylation reaction to produce propane and CO<sub>2</sub>. 2-Butanol cannot undergo the C–C bond cleavage by decarbonylation because its dehydrogenation product is a ketone and not an aldehyde.

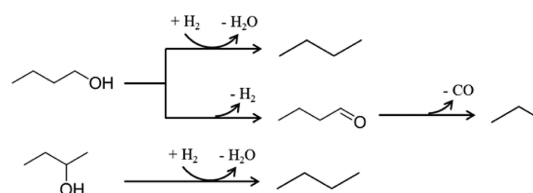


**Figure 23.** Major reaction pathways for the HDO of 1-butanol and 2-butanol over Pt/ $\text{SiO}_2$ – $\text{Al}_2\text{O}_3$  catalyst at 518 K. Redrawn with permission from ref 145. Copyright 2010 Elsevier.

#### 4.6. Mutual Influences of Oxygen-Containing Compounds during Simultaneous Reaction.

As discussed in section 2, bio-oils are complex mixtures of oxygen-containing compounds. Because of the competitive adsorption of molecules in these mixtures and subsequent inhibiting and poisoning effects, significant differences exist in reaction rates and selectivities measured from single-model compounds and from the same compound in the various mixtures. Such effects have been well recognized in studies of the mutual influence of S- and N-containing molecules during hydrotreating of petroleum-based oil.<sup>146</sup> Almost all studies of HDO of model compounds were conducted on a single compound. The few studies that investigated the inhibition effect primarily focused on the effects of H<sub>2</sub>S and water on HDO reactions over Mo-based sulfide catalysts. H<sub>2</sub>S has been found to strongly affect the activity and selectivity of the Mo-based sulfide catalysts.<sup>84,104,147–150</sup> The effect of H<sub>2</sub>S depends on the oxygenated molecule used, the experimental conditions, and the type of catalyst (Ni(Co)Mo-based catalysts). For instance, the presence of H<sub>2</sub>S strongly decreased the phenol and anisole HDO activity of the sulfided CoMo/ $\text{Al}_2\text{O}_3$  catalyst at 473 to 573 K, and the ratio of the HDO reaction pathways depended on H<sub>2</sub>S concentration.<sup>104</sup> The presence of H<sub>2</sub>S suppressed the DDO route to aromatics; however, at moderate H<sub>2</sub>S concentrations, the HYD route to alicyclics remained the same as in the absence of H<sub>2</sub>S.<sup>104</sup> A study by Bouvier et al.<sup>147</sup> on HDO of 2-ethylphenol on sulfided Mo, NiMo, and CoMo catalysts at 613 K and 7 MPa found that H<sub>2</sub>S, needed to maintain the sulfidation level of the catalysts, has promoting or inhibiting effects depending on the catalyst tested and the deoxygenation pathway considered. Over the three catalysts, H<sub>2</sub>S was found to slightly promote the HYD route and strongly inhibit the DDO route. Romeroa et al.<sup>150</sup> reported that H<sub>2</sub>S promoted the HYD route and inhibited the DDO route of 2-ethylphenol HDO over a NiMoP/ $\text{Al}_2\text{O}_3$  catalyst. In general, water caused a decrease of the catalytic activity for HDO due to competitive adsorption and modification of catalyst structure.<sup>63,65,151,152</sup> However, few studies have reported the effect of water on HDO activity of noble metal catalysts.

In addition, the mutual influence of HDO and HDS or HDN on Mo-based sulfide has been studied for simultaneous reactions during hydrotreating of petroleum-based oils<sup>153–156</sup> and coprocessing of bio-oils and petroleum-based oils.<sup>108,157</sup> For example, Philippe et al.<sup>156</sup> reported that both guaiacol and phenol inhibit the HDS of sulfur compounds (dibenzothiophene and dimethyldibenzothiophene) on a sulfided CoMoP/ $\text{Al}_2\text{O}_3$  catalyst at 613 K and 4.0 MPa. In addition, they reported that, according to a Langmuir–Hinshelwood model, guaiacol has a stronger inhibiting effect than phenol due to competitive adsorption between the oxygen- and sulfur-containing compounds on the catalyst surface. Bui et al.<sup>108</sup> observed a decrease in HDS performance of sulfided CoMo/ $\text{Al}_2\text{O}_3$  catalyst at low



temperature and high contact time during HDS processing of a straight run gas oil with coprocessing of guaiacol. This decrease in HDS was due to the formation of intermediate phenols, which compete with sulfur-containing molecules for adsorption on active sites. At a higher temperature, complete HDO of guaiacol was observed and HDS could proceed without further inhibition.

Few studies have focused on the mutual influences of oxygen-containing compounds during their simultaneous HDO reaction in the various mixtures. However, Romero et al.<sup>150</sup> studied the competitive effects between furanic compounds (benzofuran and 2,3-dihydrobenzofuran) and a phenolic compound (2-propylphenol) over a sulfided NiMoP/Al<sub>2</sub>O<sub>3</sub> catalyst at 613 K and 7 MPa in a fixed-bed reactor. Benzofuran and/or 2,3-dihydrobenzofuran strongly inhibited the transformation of 2-propylphenol into deoxygenated compounds, whereas 2-propylphenol hardly affected the conversion of benzofuran and 2,3-dihydrobenzofuran, indicating a stronger binding of benzofuran and 2,3-dihydrobenzofuran on active sites of catalysts than 2-propylphenol. Ferrari<sup>158</sup> found that a mutual competition for the HDO existed between guaiacol and ethyldecanoate. In addition, guaiacol and ethyldecanoate inhibited the conversion of 4-methylacetophenone; however, the reciprocal effect was less intense. In a brief abstract, Wan et al.<sup>159</sup> reported that results from binary combination of acetic acid and *p*-cresol on Ru/C catalyst indicated that the hydrogenation of acetic acid was suppressed by the presence of *p*-cresol. In contrast, the presence of acetic acid promoted the HDO of *p*-cresol by dehydration reaction, leading to high selectivity to methylcyclohexane. Apparently, additional studies of the HDO of bio-oil model compounds that use feed compositions more relevant to actual bio-oils are needed.

## 5. HYDROTREATING OF ACTUAL BIO-OIL FEEDS

Recently, Elliott<sup>17</sup> provided a very detailed summary of research efforts on the hydrotreating of actual bio-oil products. In addition, Choudhary<sup>20</sup> published a report in 2011 that discusses the hydroprocessing of actual bio-oils. This section focuses on recent advances in the hydrotreating of actual pyrolysis bio-oil feed, primarily on non-sulfided metal catalysts.

**5.1. One-Stage Hydrotreating of Bio-Oil with Noble Metal Catalyst.** Elliott et al.<sup>160</sup> tested Ru/C catalyst for hydrotreating of white wood pyrolysis bio-oil and bagasse pyrolysis bio-oil at 454 to 513 K, 13.2 to 14.3 MPa of H<sub>2</sub>, and 0.22 to 0.67 liquid hourly space velocity (LHSV) in a continuous-flow reactor. Table 9 compares the feed and product analysis results for bio-oil hydrotreating. For white wood oil, a deoxygenation of 31 to 70% and a product yield of

0.54 to 0.79 g/g feed (dry basis) were reported. For bagasse oil, a deoxygenation of 32 to 46% and product yield of 0.64 to 0.81 g/g feed (dry basis) were reported. Oxygen content decreased from ~42 to ~20%. Two separate phases, an aqueous phase and a tar phase, formed in the product oil because of the change in the water solubility of the component in the product oils. The products were less hydrophilic by removal of the carbonyl, olefinic, and aromatic characteristics. Significant loss of catalyst activity was observed during the experiments, probably because of coke formation and contaminants (i.e., sulfur and iron) in the bio-oil.

Wildschut et al.<sup>67</sup> investigated a variety of supported noble metal catalysts (Ru/C, Ru/TiO<sub>2</sub>, Ru/Al<sub>2</sub>O<sub>3</sub>, Pt/C, and Pd/C) for hydrotreating of beech wood pyrolysis bio-oil at temperatures of 523 and 623 K and pressures of 10 and 20 MPa in a batch reactor. In addition, typical hydrotreatment catalysts (sulfided NiMo/Al<sub>2</sub>O<sub>3</sub> and CoMo/Al<sub>2</sub>O<sub>3</sub>) were tested for comparison. Under mild HDO conditions (523 K and 10 MPa), two liquid phases (water and oil) and char were produced with mass balance varying between 77 and 96 wt %. Figure 24A shows that oil yields on a dry basis ranged between 21 and 55 wt % with oxygen contents between 18 and 27 wt %. Both the yields and the levels of deoxygenation were higher for the noble metal catalysts than for the classical hydrotreatment catalysts. For a goal of a high oil yield combined with low oxygen content, Pd/C was believed to be the best choice for mild HDO followed by Ru/TiO<sub>2</sub>. Under deep HDO conditions (623 K and 20 MPa), two oil phases were obtained with the noble metal catalysts. Mass balance ranged between 97 and 100 wt %. Figure 24B shows that the combined oil yields on a dry basis ranged between 25 and 65 wt % with oxygen contents between 6 and 11 wt %, much lower than after mild HDO. Figure 25 uses a van Krevelen plot to summarize the effects of catalyst and process conditions. Deep reduction of oxygen content seems possible only under severe conditions. Based on oil yields, deoxygenation levels, and extents of hydrogen consumption, Ru/C was suggested to be the most promising catalyst for further testing. Pd/C was considered to have the potential to provide higher oil yields than Ru/C, but with higher product oxygen content and hydrogen consumption. The deep HDO upgraded pyrolysis oil by Ru/C had lower organic acid, aldehyde, ketone, and ether content than the feed, but higher phenolic, aromatic, and alkane content. Wildschut conducted additional studies focused on using a Ru catalyst for bio-oil hydrotreating and concluded that the highest oil yield (65 wt %) at deep HDO condition was obtained for 4 h reaction time at 623 K and 20.0 MPa.<sup>68,69</sup> A longer reaction time led to a significant decrease of the oil yield due to the formation of gas products. Catalyst recycling experiments indicated a severe deactivation in hydrogenation upon recycling. Characterization of the Ru/C catalyst before and after reaction under deep HDO conditions showed significant coke deposition and a decrease in pore volume and metal dispersion.

Fisk et al.<sup>161</sup> conducted liquid phase HDO of a model bio-oil (mixture of ten compounds to reflect the composition of typical pyrolysis oil) over a series of supported Pt catalysts at 623 K in a batch reactor under inert atmosphere using in situ generated hydrogen. Pt/Al<sub>2</sub>O<sub>3</sub> showed the highest activity for deoxygenation with the oxygen content of the model oil decreasing from an initial value of 41 to 3 wt % after upgrading with oil yield of around 30% (dry basis). The major components in the treated oil were alkyl-substituted benzenes and cyclohexanes,

**Table 9. Comparison of Feed and Product Analysis Results for Bio-Oil Hydrotreating<sup>17</sup>**

	bio-oil			
	white wood	white wood, hydrogenated	bagasse	bagasse, hydrogenated
oil composition, wt % %, dry basis				
C	48.3	65.6–74.0	52.0	65.1–70.7
H	7.4	8.5–10.1	6.6	7.7–9.4
O	44.4	16.7–25.8	41.3	20.3–27.0
H/C atomic ratio (wet)	1.82	1.49–1.68	1.51	1.37–1.59
water content, wt %	30.0	9.7–15.7	35.0	11.2–14.0

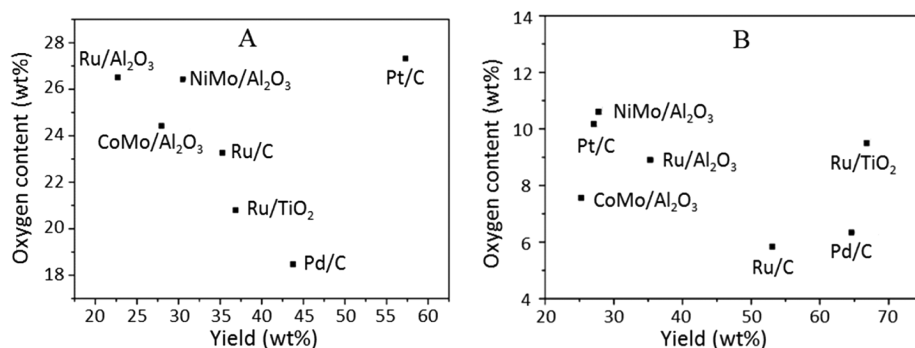


**Figure 24.** Oil yields and oxygen contents (both on a dry basis) of the combined oil phases for (A) the mild HDO of pyrolysis oil (523 K, 10.0 MPa, 4 h) and (B) deep HDO of pyrolysis oil (623 K, 20.0 MPa, 4 h) over various catalysts. Redrawn with permission from ref 67. Copyright 2009 American Chemical Society.

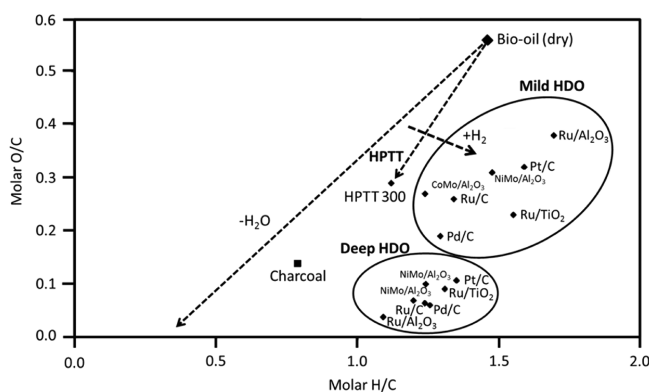


**Figure 25.** van Krevelen plot for the elemental compositions (dry basis) of the produced oils by mild (523 K, 10.0 MPa, 4 h) and deep HDO (623 K, 20.0 MPa, 4 h) with various catalysts and products by HPTT (high-pressure thermal treatment). Redrawn with permission from ref 67. Copyright 2009 American Chemical Society.

and alkyl-substituted phenols were the main residual oxygen-containing compounds. Fisk et al. suggested that the reaction route for bio-oil upgrading using in situ generated hydrogen proceeded via two steps: light oxygenates underwent reforming to H<sub>2</sub> and CO<sub>2</sub>, and, concomitantly, aromatics underwent HDO in the presence of H<sub>2</sub>.

Zhao et al.<sup>82</sup> used a bifunctional catalyst (Ni/HZSM-5) to convert *n*-hexane-extracted crude bio-oil to produce C5–C9 paraffins, naphthenes, and aromatics by a hydrogenation–hydrolysis–dehydration–dehydroaromatization cascade reaction in the presence of substantial concentrations of water at 523 K and 5 MPa of H<sub>2</sub> in a batch reactor. The components of *n*-hexane-extracted bio-oil mainly include C5–C6 substituted furans, ketones, and aldehydes and C6–C9 substituted phenols. The resulting gasoline-range hydrocarbons contain less than 10% C5–C6 paraffins and more than 90% C5–C9 naphthenes and C6–C9 aromatic molecules. The Ni/HZSM-5 catalyst was reported to be hydrothermally stable.

**5.2. Stabilization of Bio-Oil with Noble Metal Catalysts in a Dual-Stage Hydrotreating Process.** Most previously mentioned one-step hydrotreatments of bio-oil on supported metal catalysts were conducted at the high-temperature range of 523 to 623 K in batch reactors. In the test using batch reactors, bio-oil could be stabilized by hydrogenation during temperature increase from room temperature to reaction temperature, which therefore greatly alleviated the char and coke formation. However, the hydrotreating of

pyrolysis bio-oil at high temperature in a continuous-flow reactor could result in heavy product char plugging reactor and catalyst encapsulation by coke-like material, as revealed by Elliott et al.<sup>17</sup> It is notable that the industrial process for bio-oil hydrotreating prefers continuous-flow reactor. The chemical instability of bio-oil was attributed to unsaturated double bonds (e.g., olefins, aldehydes, ketones) which might react through condensation to form polymerization products. Thus, it is desirable to eliminate these groups via low-temperature hydrogenation before they react to form high-molecular-weight compounds. A two-step process was developed: a hydrotreating step at temperatures below 573 K to stabilize bio-oils, followed by the hydrotreating step at more severe conditions to achieve deep oxygen removal. Sulfide CoMo and NiMo, catalysts proven effective in producing stabilized bio-oils, have been the focus of most stabilization studies.<sup>17,20,162</sup> However, noble metals (e.g., Pd, Pt, or Ru) have also been used because of their excellent hydrogenation activity.

Gagnon and Kaliguine<sup>163</sup> investigated the effects of a mild hydrogenating pretreatment using a Ru catalyst on the HDO of wood-derived vacuum pyrolysis oil in a batch reactor. First-stage studies focused on a Ru/Al<sub>2</sub>O<sub>3</sub> catalyst at 353 to 413 K and 4–10 MPa, and second-stage studies focused on a NiO-WO<sub>3</sub>/γ-Al<sub>2</sub>O<sub>3</sub> catalyst at 623 K and 17 MPa. A temperature of 353 K and a pressure of 4 MPa were found to be the optimal conditions for the first stage. The yield of HDO products was correlated with the average molecular weight of the products. In addition to aldehyde hydrogenation and polymerization, hydrogenolysis reactions occurred over the Ru catalyst during the first stage. Gagnon and Kaliguine concluded that increased control of polymerization/coking during the less severe first-stage operating conditions resulted in higher HDO conversions.

Elliott et al.<sup>52</sup> reported that a Pd on carbon catalyst could be used in a continuous-flow reactor at 583 to 648 K, 0.18 to 1.12 LHSV, and 14 MPa to hydrogenate various bio-oils to partially upgraded bio-oils suitable for the next, more severe, hydrocracking step. Oil yield, product structure, and hydrogen consumption were not influenced dramatically by feedstock variations. Gas yield increased and oil yield decreased as temperature increased from 583 to 648 K; oxygen content reached a minimum at 613 K. Table 10 shows that oxygen content for hydrogenated bio-oil from mixed wood was 12.3 wt % (613 K and 0.25 LHSV), which was much lower than that for the feedstocks (33.7 wt %). Catalyst bed plugging was observed because of the higher temperature used in this study. The oil-phase products obtained from the first stage were further upgraded by a hydrocracking process using a traditional

**Table 10. Oil Yield and Elemental Analysis of Bio-Oil from Mixed Wood and Its Hydroprocessed Products**<sup>52</sup>

	feedstocks <sup>a</sup>	dual-stage hydroprocessed products		nonisothermal hydroprocessed products <sup>d</sup>
		hydrotreated bio-oil <sup>b</sup>	hydrocracked products <sup>c</sup>	
oil yield <sup>e</sup>		0.62	0.61	0.50
C	57.7	75.5	86.6	87.7
H	6.2	9.4	12.9	11.6
O	33.7	12.3	0.4	0.6

<sup>a</sup>Elemental composition of bio-oil was calculated on a moisture-free basis. <sup>b</sup>Pd/C catalyst, 613 K, 13.8 MPa, 0.25 LHSV. <sup>c</sup>A conventional hydrocracking catalyst, 678 K, 10.3 MPa, 0.2 LHSV. <sup>d</sup>Pd/C and hydrocracking catalyst, 523–683 K, 13.8 MPa, 0.15 LHSV. <sup>e</sup>In g/g dry feed.

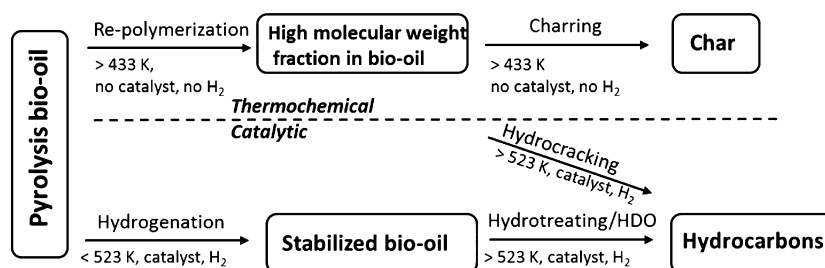
hydrocracking sulfide catalyst. The tests were performed at lower pressure (10 MPa) and higher temperature (678 K) than the hydrotreating of as-produced bio-oils, and stable operation was observed without reactor plugging, indicating that a stabilized hydrogenated bio-oil using Pd/C catalyst was suitable for severe hydrotreating. Table 10 shows that high oil yield and deep oxygen removal were achieved after the hydrocracking process. Incorporation of both steps into a nonisothermal reactor system was further explored, and, as shown in Table 10, a high yield of hydrocarbon products from the highly oxygenated bio-oil was demonstrated. A recent report by Elliott et al.<sup>164</sup> describes a two-stage hydrotreating process for upgrading the bio-oil from softwood biomass in a bench-scale continuous-flow fixed-bed reactor system. The first stage was conducted at 443 K using a carbon-supported sulfided ruthenium catalyst, and the second stage was operated at 673 K using a carbon-supported sulfided CoMo catalyst. Using this process, each gram of dry bio-oil feed yielded 0.35 to 0.45 g of oil product with densities of 0.82 to 0.92 g/mL, oxygen contents of 0.2 to 2.7 wt %, and a total acid number (TAN) of <0.01 to 2.7 mg of KOH/g. 90 to 99 h time-on-stream operations were reported using conventional bio-oil with increased pressure drop due to catalyst bed plugging by char particles in the bio-oil feedstock. The carbon-supported sulfided CoMo catalyst appeared to have limited catalyst lifetime, exhibiting deactivation over a <100 h test.

de Miguel Mercader et al.<sup>165,166</sup> focused on upgrading forest-residue pyrolysis oil by HDO over carbon-supported Ru catalysts to produce stabilized bio-oils, which can be subsequently coprocessed with refinery feed in a fluid catalytic cracking (FCC) unit. The stabilized bio-oils are required to be miscible with conventional FCC feed and can be coprocessed to produce liquid products in high yields with minimal gas/

coke production. Hydrogenation of reactive groups (e.g., olefins, aldehydes, and ketones) in bio-oils was considered critical in obtaining thermally stable feed suitable for further processing in a FCC unit. Pyrolysis oil underwent phase separation into an aqueous phase and one or two oil phases after HDO. Higher temperatures reduced the oxygen content in the product but did not affect the overall product yields (typically 50% on a dry basis). HDO conversion, based on oxygen removal, was between 57 and 67%, and the oxygen content of produced oil varied from 17 to 28 wt % on a dry basis. In spite of the relatively high oxygen content of the HDO oils, they were successfully coprocessed with a long residue in a lab-scale catalytic cracking unit without any operational problems, yielding near normal FCC gasoline and light-cycle oil products without an excessive increase in undesired coke and dry gas, as compared to the base feed only. Near oxygenate-free biohydrocarbons were obtained, probably via hydrogen transfer from the long residue. Catalytic cracking of undiluted HDO oil showed much higher yields to coke, indicating the importance of coprocessing using a refinery feed as a diluent and hydrogen transfer source.

Venderbosch et al.<sup>68,167,168</sup> studied the reaction pathways involved in the stabilization of bio-oil by mild hydrotreating using Ru catalyst. As shown in Figure 26, hydrogenation/HDO reactions were suggested to be in competition with the repolymerization reactions during hydrotreating of bio-oils. At temperatures up to 523 K, parallel reactions (i.e., repolymerization, decarboxylation, and hydrotreating) took place. The polymerization reaction rate was faster than that of hydrotreating reactions, which led to the formation of the high-molecular-weight fraction. The further polymerization of these high-molecular-weight intermediates eventually resulted in the formation of char components, which caused the reactor plugging. However, bio-oil components and the high-molecular-weight fraction formed by polymerization could be hydrotreated to produce stable bio-oil if H<sub>2</sub> and a proper catalyst were available. Venderbosch et al. suggested to steer the ratio of the heterogeneous HDO reaction to the homogeneous polymerization reaction and thereby influence product quality by optimizing operating conditions. Specifically, hydrotreating reactions could be favored over polymerization reactions by selecting the appropriate reactor (with good mixing), catalyst (with small particles), and process conditions (long residence time and low temperature).

**5.3. Hydrotreating of Aqueous Fractions of Bio-Oil with Noble Metal Catalysts.** Vispute et al.<sup>49,50</sup> reported on the hydrogenation of the aqueous fraction of wood-derived bio-oils on noble metal catalysts (e.g., Ru and Pt). The aqueous fraction of bio-oil, prepared by phase separation of bio-oil by addition of water, contained sugars, anhydrosugars, acetic acid,

**Figure 26.** Reaction routes for the hydrotreating of pyrolysis bio-oil.

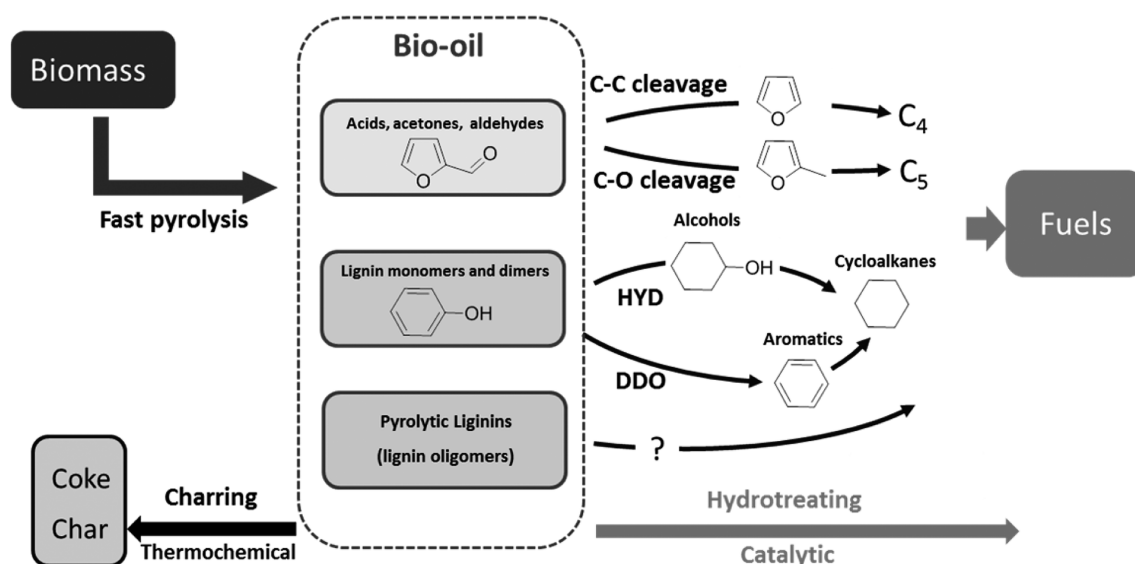


**Figure 27.** Simplified reaction routes for hydrotreating of bio-oil. DDO: direct deoxygenation. HYD: hydrogenation.

hydroxyacetone, furfural, and small amounts of guaiacols. Low-temperature hydrogenation, with a Ru/C catalyst at 398 to 448 K and 6.9 MPa in a batch reactor<sup>49</sup> or at 398 K and 5.2 to 10.0 MPa in a continuous-flow reactor,<sup>50</sup> was found to stabilize compounds with high functionalities by converting aldehydes, sugars, and unsaturated aromatics to alcohols, sugar alcohols, and saturated aromatics, respectively. The stabilized aqueous fraction was further treated by aqueous-phase reforming to produce H<sub>2</sub>,<sup>49</sup> by aqueous-phase dehydration/hydrogenation to produce alkanes,<sup>49</sup> or by zeolite upgrading to produce aromatics and olefins.<sup>50</sup> Stabilization of the aqueous fraction by hydrogenation followed by zeolite upgrading resulted in much higher yields of light alkanes, aromatics, and olefins compared to the direct upgrading of aqueous fraction of bio-oil on zeolite.<sup>50</sup> A two-stage stabilization process, involving low-temperature hydrogenation on a Ru/C catalyst at 398 K and 10.0 MPa followed by high-temperature hydrogenation on a Pt/C catalyst at 523 K and 10.0 MPa, was demonstrated to further improve the yields of light alkanes, aromatics, and olefins after zeolite upgrading.<sup>50</sup> No reactor plugging was observed in single-stage or two-stage stabilization during five days of operation, which implies that the catalysts were stable.<sup>50</sup>

Li et al.<sup>169</sup> studied the aqueous-phase HDO of carbohydrate solutions from hydrolysis of wood by a two-step catalytic process using a Ru/C catalyst at 393 K and 6.2 MPa in the first stage and a Pt/zirconium phosphate catalyst at 518 K and 6.2 MPa in the second stage. The aqueous carbohydrate solutions were a mixture of xylose, water-soluble hemicellulose oligomers, acetic acid, glucose, glucose oligomers, and probably some lignin polymers. The Ru/C catalyst was able to selectively hydrogenate xylose into xylitol but could not selectively hydrogenate the xylose oligomers. This two-stage process was able to convert the aqueous carbohydrate streams derived from maple wood into gasoline-range products with carbon yields of up to 57% and an estimated octane number of 96.5. No significant catalyst deactivation was observed, indicating that the catalysts remained very stable.

de Miguel Mercader et al.<sup>70</sup> studied the HDO of aqueous fraction of bio-oil obtained by phase separation after addition of water. They reported that operation at 493 to 583 K and 19.0 MPa on a Ru/C catalyst produced HDO oil suitable for

coprocessing with fossil feeds in a FCC unit. Compared to the oil fraction of bio-oil and the whole bio-oil, the aqueous fraction produced HDO oils with the highest quality (e.g., tendency to form coke, hydrogen/carbon ratio).

## 6. SUMMARY AND OUTLOOKS

Significant research has been conducted worldwide to discover renewable sources of energy to replace fossil fuels in the current energy system. Lignocellulosic biomass, the cheapest and most abundant biomass, has great potential to produce liquid hydrocarbons on a large-scale for the transportation sector. Several promising routes for the conversion of lignocellulosic biomass to fuels have been developed, including fast pyrolysis to bio-oil followed by upgrading, which has been identified as a simple, cost-effective, and efficient route. Bio-oils produced via fast pyrolysis of lignocellulosic biomass possess significant problems for their direct utilization because of the high oxygen content and the consequent poor quality in bio-oils. Therefore, extensive oxygen removal is required for upgrading of bio-oils to liquid transportation fuels with properties similar to those of petroleum fuels. Catalytic hydrotreating of bio-oils is the most common method to reduce the oxygen content of bio-oils and, therefore, has attracted the most attention in recent decades. The major challenge of bio-oil hydrotreating is the high oxygen content, high water content, molecular complexity, coking propensity, and corrosiveness of bio-oils, which require catalysts with high deoxygenation activity, good resistance to coke formation, and high tolerance to water and poisons to metal (e.g., sulfur- and nitrogen-containing molecules). To reduce production cost, a preferred catalyst system should also have low hydrogen consumption, a low hydrogen pressure requirement, and a high carbon yield.

Conventional Mo-based sulfide catalysts, which are most commonly used in hydrotreating in petroleum based oil refinery, have naturally been used in bio-oil hydrotreating. However, they have been identified to be unstable and sulfur must be added to the feedstream to keep the catalyst from deactivating. Recent research has focused on non-sulfide catalysts, especially noble metal catalysts. Significant advances have been made in the fundamental understanding of the chemistry of reactions taking place during bio-oil hydrotreating

on noble metal catalysts. Investigations have been performed using model compounds, primarily focusing on phenols, guaiacols, furans, furfurals, and carboxylic acids and using noble metal catalysts in the hydrotreating of actual bio-oils.

Reaction network and mechanism studies indicate three pairs of important parallel reactions taking place during hydrotreating of bio-oils that influence the stability of the catalysts, hydrogen consumption of the processes, and carbon yield in the products. Figure 27 illustrates a simplified reaction network including these reactions using the two major components of bio-oils, phenol and furfural, as examples. First, bio-oils can either form char by polymerization and charring of active molecules or form desired hydrocarbons and/or stabilized bio-oils by HDO/hydrogenation. Polymerization reactions take place faster than hydrotreating reactions at a high temperature. Therefore, a stabilization step by hydrogenation using a proper catalyst under mild conditions is required to stabilize bio-oils prior to their further upgrading. Noble metal catalysts have been widely used for the stabilization step because of their excellent hydrogenation activity. Optimization of catalysts, processes, operating conditions, and parameters will help tune the ratio of the HDO reaction to the polymerization reaction and thereby enhance catalyst stability and product quality. Second, oxygen removal from a compound containing an aromatic ring, such as phenolics (phenol in Figure 27) and furans (furfural in Figure 27), occurs via two parallel routes: direct deoxygenation (DDO route) to form aromatics or hydrogenation followed by deoxygenation (HYD route) to form saturated hydrocarbons. HDO on noble metal catalysts seems to prefer HYD over DDO under typical hydrotreating conditions because of the excellent hydrogenation activity of noble metal catalysts and the fact that cleavage of aliphatic carbon–oxygen bonds is much easier than that of aryl carbon–oxygen bonds. Nevertheless, the conditions under which the hydrogenation reaction is suppressed would lead to a higher selectivity of DDO on noble metal catalysts. However, HDO on Mo-based sulfide catalysts seems to favor DDO rather than HYD under typical hydrotreating conditions. It is desirable to avoid hydrogenation of aromatics in bio-oils and, therefore, to reduce hydrogen consumption. Third, oxygen removal from an aldehyde (such as furfural in Figure 27), a primary alcohol (the dehydrogenation product of which is an aldehyde), or a carboxylic acid occurs via C–O cleavage to H<sub>2</sub>O or by C–C cleavage to CO or CO<sub>2</sub>. The latter should be avoided to reduce carbon loss after hydrotreating of bio-oils. Further, it is desirable to avoid loss of the methyl group in the methoxyl of phenolics (e.g., anisoles and guaiacols) by a methyl transfer reaction catalyzed by acid function to further reduce carbon loss. The preference of the above parallel routes and the activity of catalyst strongly depend on the reaction conditions and the metal identity and support properties of the catalysts.

Development of a robust and optimal bio-oil hydrotreating catalyst is still a key challenge for the biomass pyrolysis-upgrading process. Desirable bio-oil hydrotreating catalyst systems are expected to achieve high HDO rates, appropriate selectivities (minimized hydrogen consumption and carbon loss), and good stability (minimized coke formation and high tolerance to water and poisons to metal). Mechanistic and structural insights, concerning the mechanisms, kinetics, and site requirements for HDO reactions on metal or metal sulfide catalysts, are required to design more effective bio-oil hydrotreating catalyst systems. Studies using simple model compounds could allow a better understanding of reaction

mechanisms and kinetics. However, gaps remain between current fundamental studies of HDO of single-model molecules and practical implementation of bio-oil hydrotreating because of the molecular complexity of bio-oils. Therefore, it is critical to conduct systemic studies for comprehensive understanding of interactions between model compounds (as individual and mixture) present in bio-oils under practical HDO conditions. High-molecular-weight compounds, including lignin-derived oligomers (pyrolytic lignins), in the bio-oil feed and oligomers of active compounds formed during hydrotreating could form char rapidly by noncatalytic polymerization and subsequently cause catalyst deactivation at typical hydrotreating conditions. Insight is needed into reaction mechanisms (both polymerization and hydrotreating) of the high-molecular-weight fraction during hydrotreating of bio-oils to design more active, selective, and stable catalysts. It is desirable to convert the high-molecular-weight fraction to stable bio-oil or target hydrocarbons by hydrotreating using appropriate catalysts and reaction conditions.

Bifunctional catalysts, including a metal function (primarily noble metals) and an acid function, have shown improved HDO activity and preferred reaction pathways compared to metal catalysts alone. Most current research on bifunctional catalysts used HDO of model compounds or treated bio-oil in batch reactors. These catalysts have great potential to be used as non-sulfide-based bio-oil hydrotreating catalysts. Additional testing is expected, including hydrotreating of actual bio-oil in continuous-flow reactors to develop next-generation catalysts.

It is also critical to test the bio-oil produced from catalytic fast pyrolysis or hydrolysis of biomass, which is expected to be more stable than conventional bio-oil and therefore to be hydrotreated with improved catalyst and operation lifetime. Another important issue is the further understanding of the catalyst deactivation mechanisms for bio-oil hydrotreating, which requires insight into the nature of active sites, mutual effect of bio-oil components, as mentioned above, and detailed catalyst characterizations. Better understanding of catalyst deactivation mechanisms would benefit the design of more stable catalysts, simpler bio-oil hydrotreating processes, and appropriate catalyst regeneration procedures.

## AUTHOR INFORMATION

### Corresponding Author

\*E-mail: Yong.Wang@pnnl.gov.

### Notes

The authors declare no competing financial interest.

## ACKNOWLEDGMENTS

This work was supported by the U.S. Department of Energy Office of Energy Efficiency and Renewable Energy Biomass program. The Pacific Northwest National Laboratory is operated by Battelle for the United States Department of Energy under Contract DE-AC05-76RL01830.

## ABBREVIATIONS

AGUs,  $\beta$ -D-anhydroglucopyranose units; BTL, biomass to liquids; CsPW, Cs<sub>2.5</sub>H<sub>0.5</sub>PW<sub>12</sub>O<sub>40</sub>; FCC, fluid catalytic cracking; GVL,  $\gamma$ -valerolactone; HDN, hydrodenitrogenation; HDO, hydrodeoxygenation; HDS, hydrodesulfurization; LHSV, liquid hourly space velocity; mTHF, methyltetrahydrofuran; TAN, total acid number

## REFERENCES

- (1) BP Statistical Review of World Energy; BP: 2011; <http://www.bp.com/sectionbodycopy.do?categoryId=7500&contentId=7068481>.
- (2) The Global Oil Depletion Report; UK Energy Research Center: 2009; <http://www.ukerc.ac.uk/support/Global%20oil%20Depletion>.
- (3) International Energy Outlook 2010; U.S. Energy Information Administration: 2010; <http://www.eia.gov/oiaf/ieo/index.html>.
- (4) BP Energy Outlook 2030; BP: 2011; <http://www.bp.com/sectiongenericarticle800.do?categoryId=9037134&contentId=7068677>.
- (5) Climate Change 2007: Synthesis Report; IPCC: 2007; [http://www.ipcc.ch/publications\\_and\\_data/publications\\_ipcc\\_fourth\\_assessment\\_report\\_synthesis\\_report.htm](http://www.ipcc.ch/publications_and_data/publications_ipcc_fourth_assessment_report_synthesis_report.htm).
- (6) Serrano-Ruiz, J. C.; Dumesic, J. A. *Energy Environ. Sci.* **2011**, *4* (1), 83–99.
- (7) Huber, G. W.; Iborra, S.; Corma, A. *Chem. Rev.* **2006**, *106* (9), 4044–4098.
- (8) Annual Energy Review; U.S. Energy Information Administration: 2010; <http://www.eia.gov/totalenergy/data/annual/#consumption>.
- (9) Klass, D. L. *Encycl. Energy* **2004**, *1*, 193–212.
- (10) Huber, G. W.; Corma, A. *Angew. Chem., Int. Ed.* **2007**, *46* (38), 7184–7201.
- (11) Huber, G. W.; Dumesic, J. A. *Catal. Today* **2006**, *111* (1–2), 119–132.
- (12) Lange, J. P. *Biofpr* **2007**, *1* (1), 39–48.
- (13) Lin, Y.-C.; Huber, G. W. *Energy Environ. Sci.* **2009**, *2* (1), 68–80.
- (14) Sutton, D.; Kelleher, B.; Ross, J. R. H. *Fuel Process. Technol.* **2001**, *73* (3), 155–173.
- (15) McKendry, P. *Bioresour. Technol.* **2002**, *83* (1), 55–63.
- (16) Elliott, D. C.; Beckman, D.; Bridgwater, A. V.; Diebold, J. P.; Gevert, S. B.; Solantausta, Y. *Energy Fuels* **1991**, *5* (3), 399–410.
- (17) Elliott, D. C. *Energy Fuels* **2007**, *21* (3), 1792–1815.
- (18) Czernik, S.; Bridgwater, A. V. *Energy Fuels* **2004**, *18* (2), 590–598.
- (19) Mohan, D.; Pittman, C. U.; Steele, P. H. *Energy Fuels* **2006**, *20* (3), 848–889.
- (20) Choudhary, T. V.; Phillips, C. B. *Appl. Catal., A* **2011**, *397* (1–2), 1–12.
- (21) Bridgwater, A. V.; Peacocke, G. V. C. *Renewable Sustainable Energy Rev.* **2000**, *4* (1), 1–73.
- (22) Simonetti, D. A.; Dumesic, J. A. *ChemSusChem* **2008**, *1* (8–9), 725–733.
- (23) Huber, G. W.; Chheda, J. N.; Barrett, C. J.; Dumesic, J. A. *Science* **2005**, *308* (5727), 1446–1450.
- (24) Anex, R. P.; Aden, A.; Kazi, F. K.; Fortman, J.; Swanson, R. M.; Wright, M. M.; Satrio, J. A.; Brown, R. C.; Dugaard, D. E.; Platon, A.; Kothandaraman, G.; Hsu, D. D.; Dutta, A. *Fuel* **2010**, *89* (Suppl. 1), S29–S35.
- (25) Yang, H.; Yan, R.; Chen, H.; Lee, D. H.; Zheng, C. *Fuel* **2007**, *86* (12–13), 1781–1788.
- (26) Ates, F.; Putun, A. E.; Putun, E. *Fuel* **2006**, *85* (12–13), 1851–1859.
- (27) Aho, A.; Kumar, N.; Eranen, K.; Salmi, T.; Hupa, M.; Murzin, D. *Fuel* **2008**, *87* (12), 2493–2501.
- (28) Carlson, T. R.; Vispute, T. R.; Huber, G. W. *ChemSusChem* **2008**, *1* (5), 397–400.
- (29) Zhang, H.; Xiao, R.; Wang, D.; Zhong, Z.; Song, M.; Pan, Q.; He, G. *Energy Fuels* **2009**, *23* (12), 6199–6206.
- (30) Carlson, T. R.; Jae, J.; Lin, Y.-C.; Tompsett, G. A.; Huber, G. W. *J. Catal.* **2010**, *270* (1), 110–124.
- (31) Zhao, Y.; Deng, L.; Liao, B.; Fu, Y.; Guo, Q. X. *Energy Fuels* **2010**, *24*, 5735–5740.
- (32) Carlson, T. R.; Cheng, Y. T.; Jae, J.; Huber, G. W. *Energy Environ. Sci.* **2011**, *4* (1), 145–161.
- (33) Mullen, C. A.; Boateng, A. A.; Mihalcik, D. J.; Goldberg, N. M. *Energy Fuels* **2011**, *25* (11), 5444–5451.
- (34) Murata, K.; Somwongsa, P.; Larpiattaworn, S.; Liu, Y.; Inaba, M.; Takahara, I. *Energy Fuels* **2011**, *25* (11), 5429–5437.
- (35) Iliopoulou, E. F.; Stefanidis, S. D.; Kalogiannis, K. G.; Delimitis, A.; Lappas, A. A.; Triantafyllidis, K. S. *Appl. Catal., B* **2012**, *127*, 281–290.
- (36) Sanna, A.; Andresen, J. M. *ChemSusChem* **2012**, *5* (10), 1944–1957.
- (37) Melligan, F.; Hayes, M. H. B.; Kwapinski, W.; Leahy, J. J. *Energy Fuels* **2012**, *26* (10), 6080–6090.
- (38) Marker, T. L.; Felix, L. G.; Linck, M. B.; Roberts, M. J. *Environ. Prog. Sustainable Energy* **2012**, *31* (2), 191–199.
- (39) Butler, E.; Devlin, G.; Meier, D.; McDonnell, K. *Renewable Sustainable Energy Rev.* **2011**, *15* (8), 4171–4186.
- (40) Oasmaa, A.; Czernik, S. *Energy Fuels* **1999**, *13* (4), 914–921.
- (41) Bridgwater, A. V. *Biomass Bioenergy* **2012**, *38*, 68–94.
- (42) Furimsky, E. *Appl. Catal., A* **2000**, *199* (2), 147–190.
- (43) Adjaye, J. D.; Bakhshi, N. N. *Fuel Process. Technol.* **1995**, *45* (3), 161–183.
- (44) Samolada, M. C.; Baldauf, W.; Vasalos, I. A. *Fuel* **1998**, *77* (14), 1667–1675.
- (45) Vitolo, S.; Seggiani, M.; Frediani, P.; Ambrosini, G.; Politi, L. *Fuel* **1999**, *78* (10), 1147–1159.
- (46) Peng, J.; Chen, P.; Lou, H.; Zheng, X. *Bioresour. Technol.* **2009**, *100* (13), 3415–3418.
- (47) Putun, E.; Uzun, B. B.; Putun, A. E. *Energy Fuels* **2009**, *23*, 2248–2258.
- (48) Stephanidis, S.; Nitsos, C.; Kalogiannis, K.; Iliopoulou, E. F.; Lappas, A. A. *Catal. Today* **2011**, *167* (1), 37–45.
- (49) Vispute, T. P.; Huber, G. W. *Green Chem.* **2009**, *11* (9), 1433–1445.
- (50) Vispute, T. P.; Zhang, H.; Sanna, A.; Xiao, R.; Huber, G. W. *Science* **2010**, *330* (6008), 1222–1227.
- (51) Topsoe, H.; Clausen, B. S.; Massoth, F. E. In *Catalysis Science and Technology*; Anderson, J. R., Boudart, M., Eds.; Springer-Verlag: New York, 1996; Vol. 11, p 1.
- (52) Elliott, D. C.; Hart, T. R.; Neuenschwander, G. G.; Rotness, L. J.; Zacher, A. H. *Environ. Prog. Sustainable Energy* **2009**, *28* (3), 441–449.
- (53) *Biomass Feedstock Composition and Property Database*; The National Renewable Energy Laboratory Laboratory: <http://www.afdc.energy.gov/biomass/progs/search1.cgi>; Content Last Updated: 05/14/2004.
- (54) Van de Vyver, S.; Geboers, J.; Jacobs, P. A.; Sels, B. F. *ChemCatChem* **2011**, *3* (1), 82–94.
- (55) Shen, D. K.; Gu, S. *Technol.* **2009**, *100* (24), 6496–6504.
- (56) Pandey, M. P.; Kim, C. S. *Chem. Eng. Technol.* **2011**, *34* (1), 29–41.
- (57) Bridgwater, A. V. *J. Anal. Appl. Pyrolysis* **1999**, *51* (1–2), 3–22.
- (58) Sipila, K.; Kuoppala, E.; Fagernas, L.; Oasmaa, A. *Biomass Bioenergy* **1998**, *14* (2), 103–113.
- (59) Branca, C.; Giudicianni, P.; Di Blasi, C. *Ind. Eng. Chem. Res.* **2003**, *42* (14), 3190–3202.
- (60) Oasmaa, A.; Elliott, D. C.; Korhonen, J. *Energy Fuels* **2010**, *24*, 6548–6554.
- (61) Hassan, E. B. M.; Steele, P. H.; Ingram, L. *Appl. Biochem. Biotechnol.* **2009**, *154* (1–3), 182–192.
- (62) Thangalazhy-Gopakumar, S.; Adhikari, S.; Ravindran, H.; Gupta, R. B.; Fasina, O.; Tu, M.; Fernando, S. D. *Bioresour. Technol.* **2010**, *101* (21), 8389–8395.
- (63) Furimsky, E.; Massoth, F. E. *Catal. Today* **1999**, *52* (4), 381–495.
- (64) Baker, E. G.; Elloitt, D. C. In *Research in Thermochemical Biomass Conversion*; Bridgwater, A. V., Kuester, J. L., Eds.; Elsevier Applied Science: Barking, U.K., 1988; p 883.
- (65) Laurent, E.; Delmon, B. *J. Catal.* **1994**, *146* (1), 281–291.
- (66) Kubicka, D.; Horacek, J. *Appl. Catal., A* **2011**, *394* (1–2), 9–17.
- (67) Wildschut, J.; Mahfud, F. H.; Venderbosch, R. H.; Heeres, H. J. *Ind. Eng. Chem. Res.* **2009**, *48* (23), 10324–10334.
- (68) Wildschut, J.; Iqbal, M.; Mahfud, F. H.; Melian-Cabrera, I.; Venderbosch, R. H.; Heeres, H. J. *Energy Environ. Sci.* **2010**, *3* (7), 962–970.

- (69) Wildschut, J.; Melian-Cabrera, I.; Heeres, H. J. *Appl. Catal., B* **2010**, *99* (1–2), 298–306.
- (70) Mercader, F. D.; Groeneveld, M. J.; Kersten, S. R. A.; Geantet, C.; Toussaint, G.; Way, N. W. J.; Schaverien, C. J.; Hogendoorn, K. J. A. *Energy Environ. Sci.* **2011**, *4* (3), 985–997.
- (71) Lin, Y.-C.; Li, C.-L.; Wan, H.-P.; Lee, H.-T.; Liu, C.-F. *Energy Fuels* **2011**, *25* (3), 890–896.
- (72) Li, K.; Wang, R.; Chen, J. *Energy Fuels* **2011**, *25* (3), 854–863.
- (73) Zhao, H. Y.; Li, D.; Bui, P.; Oyama, S. T. *Appl. Catal., A* **2011**, *391* (1–2), 305–310.
- (74) Zhao, C.; He, J.; Lemonidou, A. A.; Li, X.; Lercher, J. A. *J. Catal.* **2011**, *280* (1), 8–16.
- (75) Zhao, C.; Lercher, J. A. *ChemCatChem* **2012**, *4* (1), 64–68.
- (76) Centeno, A.; Laurent, E.; Delmon, B. *J. Catal.* **1995**, *154* (2), 288–298.
- (77) Elliott, D. C.; Hart, T. R. *Energy Fuels* **2009**, *23* (1), 631–637.
- (78) Van, N. B.; Laurenti, D.; Delichere, P.; Geantet, C. *Appl. Catal., B* **2011**, *101* (3–4), 246–255.
- (79) Chiranjeevi, T.; Kumaran, G. M.; Dhar, G. M. *Pet. Sci. Technol.* **2008**, *26* (6), 690–703.
- (80) Zhu, X.; Lobban, L. L.; Mallinson, R. G.; Resasco, D. E. *J. Catal.* **2011**, *281* (1), 21–29.
- (81) Hong, D. Y.; Miller, S. J.; Agrawal, P. K.; Jones, C. W. *Chem. Commun.* **2010**, *46* (7), 1038–1040.
- (82) Zhao, C.; Lercher, J. A. *Angew. Chem., Int. Ed.* **2012**, *51* (24), 5935–5940.
- (83) Grange, P.; Laurent, E.; Maggi, R.; Centeno, A.; Delmon, B. *Catal. Today* **1996**, *29* (1–4), 297–301.
- (84) Gevert, B. S.; Otterstedt, J. E.; Massoth, F. E. *Appl. Catal.* **1987**, *31* (1), 119–131.
- (85) Furimsky, E.; Mikhlin, J. A.; Jones, D. Q.; Adley, T. *Can. J. Chem. Eng.* **1986**, *64* (6), 982–985.
- (86) Laurent, E.; Delmon, B. *Ind. Eng. Chem. Res.* **1993**, *32* (11), 2516–2524.
- (87) Massoth, F. E.; Politzer, P.; Concha, M. C.; Murray, J. S.; Jakowski, J.; Simons, J. J. *Phys. Chem. B* **2006**, *110* (29), 14283–14291.
- (88) Romero, Y.; Richard, F.; Brunet, S. *Appl. Catal., B* **2010**, *98* (3–4), 213–223.
- (89) Talukdar, A. K.; Bhattacharyya, K. G.; Sivasanker, S. *Appl. Catal., A* **1993**, *96* (2), 229–239.
- (90) Neri, G.; Visco, A. M.; Donato, A.; Milone, C.; Malentacchi, M.; Gubitosa, G. *Appl. Catal., A* **1994**, *110* (1), 49–59.
- (91) Shin, E. J.; Keane, M. A. *J. Catal.* **1998**, *173* (2), 450–459.
- (92) Mahata, N.; Vishwanathan, V. *J. Catal.* **2000**, *196* (2), 262–270.
- (93) Diaz, E.; Mohedano, A. F.; Calvo, L.; Gilarranz, M. A.; Casas, J. A.; Rodriguez, J. J. *Chem. Eng. J.* **2007**, *131* (1–3), 65–71.
- (94) Xiang, Y.; Ma, L.; Lu, C.; Zhang, Q.; Li, X. *Green Chem.* **2008**, *10* (9), 939–943.
- (95) Zhao, C.; Kou, Y.; Lemonidou, A. A.; Li, X. B.; Lercher, J. A. *Angew. Chem., Int. Edit.* **2009**, *48* (22), 3987–3990.
- (96) Zhao, C.; Kou, Y.; Lemonidou, A. A.; Li, X. B.; Lercher, J. A. *Chem. Commun.* **2010**, *46* (3), 412–414.
- (97) Zhao, C.; Camaioni, D. M.; Lercher, J. A. *J. Catal.* **2012**, *288*, 92–103.
- (98) Wan, H.; Chaudhari, R. V.; Subramaniam, B. *Top. Catal.* **2012**, *55* (3–4), 129–139.
- (99) Yan, N.; Yuan, Y.; Dykeman, R.; Kou, Y.; Dyson, P. J. *Angew. Chem., Int. Ed.* **2010**, *49* (32), 5549–5553.
- (100) Zhao, C.; Song, W.; Lercher, J. A. *ACS Catal.* **2012**, *2* (12), 2714–2723.
- (101) Zhao, C.; Kasakov, S.; He, J.; Lercher, J. A. *J. Catal.* **2012**, *296*, 12–23.
- (102) Horacek, J.; St'avorova, G.; Kelbichova, V.; Kubicka, D. *Catal. Today* **2013**, *204*, 38–45.
- (103) Foster, A. J.; Do, P. T. M.; Lobo, R. F. *Top. Catal.* **2012**, *55* (3–4), 118–128.
- (104) Viljava, T. R.; Komulainen, R. S.; Krause, A. O. I. *Catal. Today* **2000**, *60* (1–2), 83–92.
- (105) Runnebaum, R. C.; Lobo-Lapidus, R. J.; Nimmanwudipong, T.; Block, D. E.; Gates, B. C. *Energy Fuels* **2011**, *25* (10), 4776–4785.
- (106) Laurent, E.; Delmon, B. *Appl. Catal., A* **1994**, *109* (1), 97–115.
- (107) Ferrari, M.; Bosmans, S.; Maggi, R.; Delmon, B.; Grange, P. *Catal. Today* **2001**, *65* (2–4), 257–264.
- (108) Bui, V. N.; Toussaint, G.; Laurenti, D.; Mirodatos, C.; Geantet, C. *Catal. Today* **2009**, *143* (1–2), 172–178.
- (109) Van, N. B.; Laurenti, D.; Afanasiev, P.; Geantet, C. *Appl. Catal., B* **2011**, *101* (3–4), 239–245.
- (110) Gutierrez, A.; Kaila, R. K.; Honkela, M. L.; Slioor, R.; Krause, A. O. I. *Catal. Today* **2009**, *147* (3–4), 239–246.
- (111) Bykova, M. V.; Ermakov, D. Y.; Kaichev, V. V.; Bulavchenko, O. A.; Saraev, A. A.; Lebedev, M. Y.; Yakovlev, V. A. *Appl. Catal., B* **2012**, *113*, 296–307.
- (112) Nimmanwudipong, T.; Runnebaum, R. C.; Block, D. E.; Gates, B. C. *Catal. Lett.* **2011**, *141* (6), 779–783.
- (113) Nimmanwudipong, T.; Runnebaum, R. C.; Block, D. E.; Gates, B. C. *Energy Fuels* **2011**, *25*, 3417–3427.
- (114) Nimmanwudipong, T.; Aydin, C.; Lu, J.; Runnebaum, R. C.; Brodwater, K. C.; Browning, N. D.; Block, D. E.; Gates, B. C. *Catal. Lett.* **2012**, *142* (10), 1190–1196.
- (115) Runnebaum, R. C.; Nimmanwudipong, T.; Block, D. E.; Gates, B. C. *Catal. Sci. Technol.* **2012**, *2* (1), 113–118.
- (116) Olcese, R. N.; Bettahar, M.; Petitjean, D.; Malaman, B.; Giovannella, F.; Dufour, A. *Appl. Catal., B* **2012**, *115*, 63–73.
- (117) Strassberger, Z.; Alberts, A. H.; Louwerse, M. J.; Tanase, S.; Rothenberg, G. *Green Chem.* **2013**, *15* (3), 768–774.
- (118) Furimsky, E. *Appl. Catal.* **1983**, *6* (2), 159–164.
- (119) Furimsky, E. *Ind. Eng. Chem. Prod. Res. Dev.* **1983**, *22* (1), 31–34.
- (120) Bunch, A. Y.; Wang, X. Q.; Ozkan, U. S. *J. Mol. Catal. A: Chem.* **2007**, *270* (1–2), 264–272.
- (121) LaVopa, V.; Satterfield, C. N. *Energy Fuels* **1987**, *1* (4), 323–331.
- (122) Kiewer, C. J.; Aliaga, C.; Bieri, M.; Huang, W.; Tsung, C.-K.; Wood, J. B.; Komvopoulos, K.; Somorjai, G. A. *J. Am. Chem. Soc.* **2010**, *132* (37), 13088–13095.
- (123) Kreuzer, K.; Kramer, R. *J. Catal.* **1997**, *167* (2), 391–399.
- (124) Liu, C.; Shao, Z.; Xiao, Z.; Williams, C. T.; Liang, C. *Energy Fuels* **2012**, *26* (7), 4205–4211.
- (125) Bowker, R. H.; Smith, M. C.; Pease, M. L.; Slenkamp, K. M.; Kovarik, L.; Bussell, M. E. *ACS Catal.* **2011**, 917–922.
- (126) Rao, R.; Baker, R.; Vannice, M. *Catal. Lett.* **1999**, *60* (1), 51–57.
- (127) Kijeński, J.; Winiarek, P.; Paryjczak, T.; Lewicki, A.; Mikołajska, A. *Appl. Catal., A* **2002**, *233* (1–2), 171–182.
- (128) Li, H.; Luo, H.; Zhuang, L.; Dai, W.; Qiao, M. *J. Mol. Catal. A: Chem.* **2003**, *203* (1–2), 267–275.
- (129) Zheng, H.-Y.; Zhu, Y.-L.; Teng, B.-T.; Bai, Z.-Q.; Zhang, C.-H.; Xiang, H.-W.; Li, Y.-W. *J. Mol. Catal. A: Chem.* **2006**, *246* (1–2), 18–23.
- (130) Sitthisa, S.; Sooknoi, T.; Ma, Y. G.; Balbuena, P. B.; Resasco, D. E. *J. Catal.* **2011**, *277* (1), 1–13.
- (131) Sitthisa, S.; Resasco, D. *Catal. Lett.* **2011**, *141* (6), 784–791.
- (132) Sitthisa, S.; Pham, T.; Prasomsri, T.; Sooknoi, T.; Mallinson, R. G.; Resasco, D. E. *J. Catal.* **2011**, *280* (1), 17–27.
- (133) Zhang, W.; Zhu, Y.; Niu, S.; Li, Y. *J. Mol. Catal. A: Chem.* **2011**, *335* (1–2), 71–81.
- (134) Pestman, R.; Koster, R. M.; Pieterse, J. A. Z.; Ponec, V. *J. Catal.* **1997**, *168* (2), 255–264.
- (135) Pestman, R.; Koster, R. M.; Boellaard, E.; van der Kraan, A. M.; Ponec, V. *J. Catal.* **1998**, *174* (2), 142–152.
- (136) Rachmady, W.; Vannice, M. A. *J. Catal.* **2000**, *192* (2), 322–334.
- (137) Rachmady, W.; Vannice, M. A. *J. Catal.* **2002**, *208* (1), 158–169.
- (138) Rachmady, W.; Vannice, M. A. *J. Catal.* **2002**, *207* (2), 317–330.

- (139) Gursahani, K. I.; Alcalá, R.; Cortright, R. D.; Dumesic, J. A. *Appl. Catal., A* **2001**, 222 (1–2), 369–392.
- (140) Olcay, H.; Xu, L. J.; Xu, Y.; Huber, G. W. *ChemCatChem* **2010**, 2 (11), 1420–1424.
- (141) Pallassana, V.; Neurock, M. *J. Catal.* **2002**, 209 (2), 289–305.
- (142) Alotaibi, M. A.; Kozhevnikova, E. F.; Kozhevnikov, I. V. *Appl. Catal., A* **2012**, 447, 32–40.
- (143) Chen, L.; Zhu, Y.; Zheng, H.; Zhang, C.; Li, Y. *Appl. Catal., A* **2012**, 411, 95–104.
- (144) Wildschut, J.; Arentz, J.; Rasrendra, C. B.; Venderbosch, R. H.; Heeres, H. J. *Environ. Prog. Sustainable Energy* **2009**, 28 (3), 450–460.
- (145) Li, N.; Huber, G. W. *J. Catal.* **2010**, 270 (1), 48–59.
- (146) Egorova, M.; Prins, R. J. *Catal.* **2004**, 221 (1), 11–19.
- (147) Bouvier, C.; Romero, Y.; Richard, F.; Brunet, S. *Green Chem.* **2011**, 13, 2441–2451.
- (148) Senol, O. I.; Ryymin, E. M.; Viljava, T. R.; Krause, A. O. I. *J. Mol. Catal. A: Chem.* **2007**, 277 (1–2), 107–112.
- (149) Ferrari, M.; Maggi, R.; Delmon, B.; Grange, P. *J. Catal.* **2001**, 198 (1), 47–55.
- (150) Romero, Y.; Richard, F.; Renème, Y.; Brunet, S. *Appl. Catal., A* **2009**, 353 (1), 46–53.
- (151) Laurent, E.; Delmon, B. In *Catalyst Deactivation*; Delmon, B., Froment, G. F., Eds.; Elsevier: Amsterdam, 1994; Vol. 88, p 459.
- (152) Senol, O. I.; Viljava, T. R.; Krause, A. O. I. *Catal. Today* **2005**, 106 (1–4), 186–189.
- (153) Odebunmi, E. O.; Ollis, D. F. *J. Catal.* **1983**, 80 (1), 65–75.
- (154) Odebunmi, E. O.; Ollis, D. F. *J. Catal.* **1983**, 80 (1), 76–89.
- (155) Viljava, T. R.; Komulainen, S.; Selvam, T.; Krause, A. O. I. In *Hydrotreatment and Hydrocracking of Oil Fractions*; Delmon, B., Froment, G. F., Grange, P., Eds.; Elsevier: Amsterdam, 1999; Vol. 127, p 145.
- (156) Philippe, M.; Richard, F.; Hudebine, D.; Brunet, S. *Appl. Catal., A* **2010**, 383 (1–2), 14–23.
- (157) Pinheiro, A.; Hudebine, D.; Dupassieux, N.; Geantet, C. *Energy Fuels* **2009**, 23 (1), 1007–1014.
- (158) Ferrari, M.; Bosmans, N.; Lahousse, C.; Maggi, R.; Delmon, B. In *Biomass for energy and industry, Proceedings of the 10<sup>th</sup> European conference*; Webar, K. H., Palz, W., Chartier, P., Ferrero, G. L., Eds.; C.A.R.M.E.N.: Rimpfing, Germany, 1998; p 1658.
- (159) Wan, H.; Raghunath, V. C.; Subramaniam, B. *Catalytic Hydroprocessing of Fast Pyrolysis Bio-oil Model Compounds*; 2011 AIChE Annual Meeting, Minneapolis, MN, 2011.
- (160) Elliott, D. C.; Neuenschwander, G. G.; Hart, T. R.; Hu, J.; Solana, A. E.; Cao, C. In *Thermal and Chemical Biomass Conversion*; Bridgwater, A. V., Boocock, D. G. B., Eds.; CPL Press: Newbury, U.K., 2006; Vol. 2, p 1536.
- (161) Fisk, C. A.; Morgan, T.; Ji, Y.; Crocker, M.; Crofcheck, C.; Lewis, S. A. *Appl. Catal., A* **2009**, 358 (2), 150–156.
- (162) French, R. J.; Hrdlicka, J.; Baldwin, R. *Environ. Prog. Sustainable Energy* **2010**, 29 (2), 142–150.
- (163) Gagnon, J.; Kaliaguine, S. *Ind. Eng. Chem. Res.* **1988**, 27 (10), 1783–1788.
- (164) Elliott, D. C.; Hart, T. R.; Neuenschwander, G. G.; Rotness, L. J.; Olarte, M. V.; Zacher, A. H.; Solantausta, Y. *Energy Fuels* **2012**, 26 (6), 3891–3896.
- (165) de Miguel Mercader, F.; Groeneveld, M. J.; Kersten, S. R. A.; Way, N. W. J.; Schaverien, C. J.; Hogendoorn, J. A. *Appl. Catal., B* **2010**, 96 (1–2), 57–66.
- (166) de Miguel Mercader, F.; Koehorst, P. J. J.; Heeres, H. J.; Kersten, S. R. A.; Hogendoorn, J. A. *AIChE J.* **2011**, 57 (11), 3160–3170.
- (167) Venderbosch, R. H.; Ardiyanti, A. R.; Wildschut, J.; Oasmaa, A.; Heeres, H. J. *J. Chem. Technol. Biotechnol.* **2010**, 85 (5), 674–686.
- (168) Oasmaa, A.; Kuoppala, E.; Ardiyanti, A.; Venderbosch, R. H.; Heeres, H. J. *Energy Fuels* **2010**, 24, 5264–5272.
- (169) Li, N.; Tompsett, G. A.; Zhang, T. Y.; Shi, J. A.; Wyman, C. E.; Huber, G. W. *Green Chem.* **2011**, 13 (1), 91–101.